NATIONAL ADVISORY COMMITTEE FOR AERONAUTICS

TECHNICAL NOTE 3181

EXPERIMENTAL INVESTIGATION OF HEAT-TRANSFER AND FLUID-FRICTION CHARACTERISTICS OF WHITE FUMING NITRIC ACID

By Bruce A. Reese and Robert W. Graham

Purdue University

Washington

May 1954

NATIONAL ADVISORY COMMITTEE FOR AERONAUTICS

TECHNICAL NOTE 3181

EXPERIMENTAL INVESTIGATION OF HEAT-TRANSFER AND FLUID-FRICTION CHARACTERISTICS OF WHITE FUMING NITRIC ACID

By Bruce A. Reese and Robert W. Graham

SUMMARY

As part of the general rocket-research program of the National Advisory Committee for Aeronautics, experiments have been conducted to determine the heat-transfer and fluid-friction characteristics of white fuming nitric acid over the following range of conditions:

Heat-flux density, Btu/(sq in.)(sec)	0.13 - 1.4
Pressure, lb/sq in. abs	64 - 165
Acid inlet temperature, ^{o}F	50 - 137
Reynolds number	55,000 - 220,000

In the forced-convection regime (without surface boiling) the Fanning friction coefficient with heat transfer f_q can be satisfactorily related to the isothermal friction coefficient f_{iso} measured at the same Reynolds number by the following equation:

$$\frac{f_{iso}}{f_q} = \left(\frac{\mu_{bulk}}{\mu_{wall}}\right)^{0.12}$$

where μ is the viscosity of the white fuming nitric acid.

The heat-transfer results are satisfactorily correlated by the following equation:

$$j = 0.023\ N_{Re}^{-0.2}$$

where j is the Colburn factor, N_{Re} is Reynolds number, and all physical properties are evaluated at the bulk temperature.

Some preliminary results are presented for the regime of forced convection with nucleate boiling.

INTRODUCTION

In recent years a number of investigations have been conducted on heat transfer to liquids where large temperature gradients occurred at the heated surface. (Some of these investigations are reported in refs. 1 to 16.) In the design and operation of regeneratively cooled rocket motors it is desirable to have an accurate knowledge of the heat-transfer and pressure-drop characteristics of the liquid coolant. The correlations based on convective heat-transfer measurements at low heat-flux densities have not been considered adequate for the prediction of the convective heat transfer at the high heat-flux densities encountered in regeneratively cooled rocket motors. The heat-transfer characteristics of a few of the rocket propellants employed as coolants have been investigated and reported in the literature (refs. 1 to 3).

As part of its general rocket-research program the National Advisory Committee for Aeronautics initiated an experimental investigation at Purdue University Rocket Laboratory on the behavior of white fuming nitric acid (commercial anhydrous nitric acid, hereafter designated as WFNA) as a coolant and the results obtained are reported herein. This investigation was carried out under the sponsorship and with the financial assistance of the NACA. An investigation of the heat-transfer and pressure-drop characteristics of WFNA was particularly desirable because the WFNA decomposes even at room temperatures. Consequently it was not at all certain that the heat-transfer correlation equations derived for pure liquids at low heat-flux densities could be employed for calculating the heat-transfer coefficients for WFNA at high heat-flux densities because of the possibility of the composition of the WFNA changing with heat addition; in decomposing the WFNA yields oxides of nitrogen and water. From the more fundamental point of view of studying heat transfer per se, WFNA is an unsatisfactory liquid which introduces appreciable experimental difficulties because of its corrosivity and uncertainties regarding its physical properties.

A 0.539-inch-inside-diameter tube 24 inches long fabricated from Haynes-Stellite Alloy 25 was utilized as the test section, which was employed as a resistance element heated by alternating current and cooled by the WFNA flowing through it. Experimental data were taken over a wide range of operating conditions: Reynolds numbers from 55,000 to 220,000, heat-flux densities ranging from 0.13 to 1.4 Btu/(sq in.)(sec), system pressures from 64 to 165 lb/sq in. abs, and inlet WFNA temperatures from 51° to 137° F. Most of the heat-transfer data were in the forced-convection (without surface boiling) regime, but some preliminary investigations were made in the forced-convection region where the surface temperature of the test section exceeded the indicated boiling point (surface boiling) of the WFNA. Accurate data on heat transfer with surface boiling are of considerable interest since investigations with water

in this regime indicate that heat-flux densities up to 8 Btu/(sq in.)(sec) can be absorbed by the coolant. Heat-transfer rates of this order of magnitude are now being encountered in the research being conducted at the Purdue University Rocket Laboratory concerned with the operation of rocket motors at abnormally high combustion pressures (ref. 17).

Acknowledgment is due Dr. M. J. Zucrow, project director, for his continuous assistance throughout the project and for his help in the preparation of this report. The authors would also like to express their gratitude for the wholehearted cooperation they have received from the NACA staff, both in Washington, D. C., and at the Lewis Flight Propulsion Laboratory, Cleveland, Ohio.

SYMBOLS

A	area, sq ft, sq in.
C	constant
c_p	specific heat at constant pressure, Btu/(lb)($^\circ$F)
D	diameter, ft, in.
f	Fanning friction factor
G	weight rate of flow, lb/hr, lb/sec
g	gravity constant, 32.174 ft/sec^2
h	surface coefficient of heat transfer, Btu/(sq ft)(hr)($^\circ$F), Btu/(sq in.)(sec)($^\circ$F)
j	Colburn factor
k	thermal conductivity, Btu/(ft)(hr)($^\circ$F), Btu/(in.)(sec)($^\circ$F)
L	length, ft
M	weight flow rate per unit area, lb/(hr)(sq ft)
N_{Nu}	Nusselt number, hD/k
N_{Pr}	Prandtl number, $c_p\mu/k$
N_{Re}	Reynolds number, $\rho DV/\mu$

Δp	frictional pressure drop or pressure drop across orifice, lb/sq in.
P	pressure, lb/sq in. abs
q	heat transferred per unit time, Btu/hr, Btu/sec
R_i	radius of inside of tube, ft
R_o	radius of outside of tube, ft
t	bulk or mixing-cup temperature, ^oF
t_o	outside surface temperature of test section, ^oF
t_s	surface or inside tube-wall temperature, ^oF
t_{sat}	saturation temperature, ^oF
Δt_x	excess temperature, $t_s - t_{sat}$, ^oF
V	velocity, ft/sec
x	distance from inlet
γ	specific weight, lb/ft^3
μ	viscosity, lb/(ft)(sec)
ρ	density

Subscripts:

bulk	properties evaluated at bulk temperature
iso	isothermal
m	metal
mean	mean value
q	nonisothermal
s	inside surface or wall of tube
wall	measured at inside surface of wall

1 inlet

2 outlet

Superscripts:

m constant

n constant

APPARATUS AND INSTRUMENTATION

The design and arrangement of the apparatus and instrumentation employed in the investigation are discussed in detail in reference 18. Only a brief description is, therefore, presented here.

Figure 1 is a schematic diagram of the electrically heated test section and the associated equipment. Referring to figure 1 the flow through the apparatus is as follows. The pump A circulates the acid in the closed system. The flow was regulated by the remotely controlled air-operated Annin throttle valve C and the hand-operated bypass valve B. The flow was metered by the calibrated sharp-edge orifice D with the differential pressure being determined by means of a Wiancko differential pressure transducer and a hand-balanced potentiometer. The small tank E was installed for reducing pressure and flow fluctuations and for convenience in pressurizing the flow circuit.

Two Annin throttle valves F and J were installed at the upstream and downstream ends of the test section as a safety feature; controls were incorporated for closing the valves rapidly in the event of a test-section rupture. The two mixing chambers located upstream and downstream from the test sections comprise three concentric tubes arranged so that the acid makes three passes longitudinally through the mixing chamber before its temperature is measured. This design of the mixing chamber assures that the thermocouple reads the bulk (mixing cup) temperature. To obtain a fully developed isothermal boundary layer and a uniform turbulent velocity profile for the WFNA entering the test section a starting length of tube equal to approximately 25 tube diameters was inserted between the upstream mixing chamber and the test section. A straight length of tube equal to approximately 10 tube diameters is employed between the test section and the downstream mixing chamber to insure smooth flow leaving the test section.

The test section H is a Haynes-Stellite Alloy 25 tube having an outside diameter of 5/8 inch, a wall thickness of 0.043 inch, and a total length of 24 inches. Figure 2 presents the details of the installation

of the test section in the WFNA flow circuit. The outside wall temperatures of the test section were measured at 14 locations (see fig. 2(c)) with Chromel-Alumel thermocouples (30 gage wire) and an automatic self-balancing indicating-type Brown potentiometer. The pressure drop over the length of the test section was measured by utilizing a Wiancko differential pressure transducer. The test section was insulated thermally by a 1/2-inch layer of Sauereisen cement and 12 inches of glass wool with two concentric aluminum-foil radiation shields spaced at radii of 2 and 6 inches approximately. The glass wool and aluminum also surrounded the tubes which connected the mixing chambers to the test section.

The test section was heated with alternating current, the tube acting as a resistance element, and the WFNA cooled the test section by forced convection. Power was supplied to the test section from a 240-volt alternating-current single-phase generator and a multitap transformer having a maximum power rating of 100 kilowatts. Because of the maximum current limitation of the multitap transformer (2,500 amps) and the resistance of the test section the maximum utilizable power for heating was 67 kilowatts.

The heat added to the WFNA after flowing through the test section was removed in the double-tube aluminum heat exchanger K, which enabled one to maintain a constant temperature for the WFNA entering the test section. Valves M, N, and P were provided for draining the system and flushing it with either air or water. The system is filled with WFNA by forcing the WFNA out of the storage tank Q with low-pressure nitrogen gas.

The WFNA flow system and instrumentation described in reference 18 performed satisfactorily in preliminary trials made with water as the test fluid. After some exploratory experiments with WFNA it was necessary to make the following changes:

(1) The thermocouples in the mixing chambers were changed from Chromel-Alumel to copper-constantan thermocouples (30 gage); the copper-constantan couples were found to be more suitable for the range of WFNA temperatures encountered.

(2) The thermocouples were silver-soldered to the outside surface of the test section instead of using the condenser discharge method for attaching them; the condenser discharge method caused the thermocouples to become so brittle that they broke quite readily. The silver-solder method consisted of drilling a hole 0.005 inch deep with a number 40 drill, filling the depression with silver solder, melting the silver solder, and then quickly inserting the thermocouple in the molten solder. This method for attaching the thermocouples produced a strong junction at the surface of the tube and had no discernible effect upon the properties of the thermocouple wire.

(3) The annular-ring method for measuring the static pressure at the entrance and exit of the test section had to be abandoned because of electric current being conducted by the WFNA across the small gap between the flanges which caused the weld that attached the Van Stone ring to the tube to burn through, thus producing leakage of WFNA. The pressure taps employed in all of the experiments consisted of 1/16-inch holes drilled through the flanges of the mixing chambers that were attached to the test section. Figure 2(a) shows the position of the drilled holes and indicates by means of dotted lines the discarded method for measuring the static pressure. The drilled holes are located approximately 1/2 inch from the ends of the test section, but the corrections for the unheated portion of the connecting tubes are relatively simple to make.

(4) After the method for measuring static pressure was changed (see (3) above) the life of the test section was increased. It was found, however, that electric current was still being conducted through the WFNA from the test section to the mixing chamber and burning through the weld that attached the Van Stone ring. To reduce the flow of electric current the mixing chambers were insulated electrically from the rest of the WFNA flow circuit. Electrical insulation of the mixing chambers from the rest of the circuit reduced the rate of burning at the ends of the test section by arcing, but did not eliminate it entirely.

(5) The Statham differential pressure transducers, which functioned satisfactorily for a long period of time over a wide range of conditions when water was used as the coolant, failed to operate after only short exposure to the WFNA probably because of corrosion. Replacement Statham units also failed after short exposure to the WFNA. Since Wiancko differential pressure transducers had been used successfully at the Purdue University Rocket Laboratory for WFNA flow and pressure measurements, the Statham transducers were replaced by Wiancko transducers. The Wiancko transducers performed satisfactorily in the WFNA circuit, the only difficulty encountered being slight change in the zero (no differential pressure) reading with time, pressure, and temperature; consequently it was necessary to read the zeros at frequent intervals.

PRELIMINARY TESTS AND PROCEDURE

A number of preliminary investigations were conducted to check the instrumentation.

Measurement of Weight Flow

The Statham differential pressure transducers were calibrated against a mercury manometer. Employing the Statham unit as the differential

pressure gage, the sharp-edge orifice in the WFNA flow circuit was calibrated in position. Water from the cooling-system supply tank was pumped through the WFNA flow circuit and weighed as it discharged from that circuit.

Measurement of Bulk Temperature

The copper-constantan thermocouples employed for the measurement of the bulk temperature of the WFNA were calibrated in a furnace against a standardized platinum - platinum-rhodium thermocouple. The deviations from the standard were negligible.

Measurement of Surface Temperature of Test Section

The temperatures of the outside surface of the test section were read on a 20-point-indicating Brown automatic self-balancing potentiometer. When the tube was heated with alternating-current power it was found that the indicating dial of the Brown potentiometer slowly oscillated (approximately 1/2 cycle per second) when connected to those thermocouples attached at the ends of the test section; the amplitude of the oscillations increased with increasing temperature to approximately ±20° F at 500° F. The thermocouples near the center of the test section, however, always gave steady readings. The temperature readings of the thermocouples located at the end of the test section when measured with a hand-balanced potentiometer were always steady. Oscilloscope measurements of these same thermocouples showed both a 60- and 900-cycle alternating-current pickup from the thermocouples. It was not possible to eliminate the oscillations of the Brown potentiometer dial but it was found experimentally that the average of the maximum and minimum readings of the dial gave the correct values of surface temperature.

In an effort to locate the source of the oscillations the magnetic field around the test section was investigated by placing a loop of wire connected to a sensitive galvanometer at a number of positions. No field was detected that had sufficient strength to influence the temperature readings.

Heat Losses

The heat loss from the insulated test section was obtained for two different average wall temperatures by supplying power to the test section without liquid in the system. After equilibrium conditions had been maintained for 1 hour the power input and all test-section outer surface temperatures were recorded. At an average surface temperature of 240° F the power loss was 5 watts and at an average surface temperature

of 450° F the power loss was 11.3 watts. The corresponding heat loss was always less than 0.1 percent of the power supplied to the test section during any heat-transfer experiment and was, therefore, neglected in calculating heat-transfer coefficients.

Heat-Transfer Test With Water

Heat-transfer tests with water were conducted to test the apparatus and the experimental procedure. The results, which covered a Reynolds number range of 49,500 to 166,000 with heat-flux densities up to 0.76 Btu/(sq in.)(sec), were satisfactorily correlated by the equation of Kaufman and Isely (ref. 4):

$$N_{Nu} = 0.0168 \left(N_{Re}\right)^{0.84} \left(N_{Pr}\right)^{0.4}$$

Heat-Transfer Tests With WFNA

Before conducting the heat-transfer experiments with WFNA, the modifications to the apparatus discussed in the section entitled "Apparatus and Instrumentation" were made. The detailed steps of the experimental procedure were as follows: (1) The cooling water was circulated through the aluminum heat exchanger; (2) the acid system was filled and pressurized to the desired value; (3) the zero readings were taken for the Wiancko units; (4) the acid pump was started and the acid flow was regulated to a predetermined value; and (5) the motor generator set was started and electric power was applied to the test section.

After thermal equilibrium was established, readings were taken of the outside surface temperatures of the test section, the bulk temperatures of the acid entering and leaving the test section, the electrical power supplied to the test section, the inlet pressure to the test section, the acid flow rate, and the pressure drop across the length of the test section.

In most of the experiments the electrical power supplied to the test section was varied while the WFNA flow rate and inlet temperature were maintained relatively constant. At the completion of each series of such trials the electrical power and the acid pump were shut down and the zeros of the Wiancko units were read. For the tests with the higher acid inlet temperatures the flow of the cooling water in the aluminum heat exchanger was reduced until the acid temperature was raised to the desired value by the electrical power supplied to the test section. The cooling-water flow rate was then adjusted until thermal equilibrium was established at the desired WFNA inlet temperature.

METHOD OF CALCULATION

The calculations in this investigation were carried out on IBM machines at the Purdue Statistical Laboratory. The method of calculation, the important equations, the physical-property data, and an estimate of the accuracy of the results are given below.

Temperatures

Since the following heat-transfer coefficients were desired, (a) average over-all value for the test section and (b) the local values at seven positions along the test section, it was necessary to compute (1) the average temperature of the outside surface of the test section and (2) the average temperature for the two thermocouples employed for measuring the local value of the surface temperature at each of the seven positions. The average temperature of the outside surface of the test section, denoted by t_o, was determined by integrating numerically the measured temperature along its surface as a function of the test-section length. The temperatures used in the integration were the average of the two thermocouples located 180° apart at each of the seven stations along the test section.

The average temperature of the inside surface of the test section denoted by t_s was calculated from the following equation (ref. 19):

$$t_s = t_o - \frac{q}{2\pi L\, k_m \left(R_o^2 - R_i^2\right)} \left(R_o^2 \log_e \frac{R_o}{R_i} - \frac{R_o^2 - R_i^2}{2} \right) \qquad (1)$$

It was assumed in deriving equation (1) that the heat was generated uniformly across the tube wall and that all of the heat flow was radially inward. Substituting the values of $R_o = 0.625$ inch, $R_i = 0.539$ inch, and $L = 24$ inches into equation (1) gives

$$t_s = t_o - 0.00617 \frac{q}{k_m} \qquad (2)$$

where q is the electrical power supplied to the test section in British thermal units per hour.

Equations (1) and (2) may be corrected to include the effect of the variation of electrical resistivity with temperature (see refs. 5 and 18), but since these data are not available it was not felt that the experimental work necessary to obtain these data was justified because of the

absence of precise data for the thermal conductivity of the metal and for the physical properties of WFNA.

The heat loss from the test section was so small (see the section entitled "Preliminary Tests") that the measured value of q, with no correction for heat loss, was utilized as the heat transferred to the WFNA. The values of thermal conductivity of Haynes-Stellite Alloy 25 used in equation (2) are presented in figure 3. The thermal conductivity k_m of the alloy was determined experimentally at 145° F. The slope of the curve from the measured value was extrapolated from published data on the thermal conductivity of several other similar Haynes-Stellite alloys (ref. 20). The temperature employed for determining the value of k_m from figure 3 was the average tube-wall temperature $(t_o + t_s)/2$.

Equations were derived for the curves presenting the thermal conductivity of Haynes-Stellite Alloy 25 as a function of temperature and all the physical properties of WFNA as a function of temperature. These equations were converted into coded instructions for use in the IBM machine calculations.

The average bulk temperature t of the WFNA utilized in calculating the average over-all heat-transfer coefficient and the Fanning friction factor was assumed to be the arithmetic mean of the bulk temperatures of the acid entering the test section t_1 and that leaving the test section t_2.

In calculating the local heat-transfer coefficients the arithmetic average of the readings of two thermocouples 180° apart was used for t_o; the inside surface temperature t_s was calculated by means of equation (2). In calculating the bulk temperature of the acid for each of the seven stations it was assumed that the WFNA temperature increased linearly from the inlet to the outlet of the test section.

Heat-Transfer Coefficient

The heat-transfer coefficient h was calculated from the equation

$$h = \frac{q}{A(t_s - t)} \tag{3}$$

where q is the electric power supplied to the tube in British thermal units per hour and A is the inside surface area of the test section in square feet.

Fanning Friction Coefficient

The friction data were evaluated from the observed pressure drop across the length of the test section with and without heat addition. The momentum pressure loss across the test section was insignificant; thus, no attempt was made to correct the observed pressure-drop readings for the momentum pressure loss. Average Fanning friction coefficients for the test section were calculated from the observed data by employing the following equation:

$$f = \frac{\Delta p g \gamma A^2 D}{2G^2 L} \qquad (4)$$

Physical Properties of WFNA

All of the physical properties of WFNA employed in calculating the dimensionless groups N_{Re}, N_{Pr}, and N_{Nu}, with the exception of the specific heat, were determined at Purdue University under the sponsorship of the NACA (see ref. 21). The physical-property data are presented in figures 1 to 4 of reference 21 as functions of temperature. The Prandtl modulus is presented in figure 6 of reference 21. The error in the values of the specific heat of WFNA is unknown. The maximum errors in the viscosity measurements are judged to be of the order of 5 percent at 300° F and less than 1 percent at room temperature. The error in the density determinations is judged to be approximately 0.2 percent in the region below 100° F and approximately 4 percent at 300° F. The thermal-conductivity measurements are judged to be within 5 percent (up to 122° F) of the correct value. The extrapolation of the latter data to 300° F is probably of the same order of accuracy.

Estimated Accuracy of Calculated Results

The factor contributing the greatest probability of error in the values of the heat-transfer coefficient is the determination of the inside surface temperature of the test section. The thermocouples were silver-soldered in a small hole approximately 0.005 inch deep. It is probable that the temperature of the silver solder which is measured by the thermocouple is somewhat lower than the outside temperature of the test section. The maximum probable error in measuring the outside surface temperature of the test section is approximately -4 percent of the temperature drop through its wall. Experiments were conducted that justified the assumptions made in deriving equation (2), which was employed for calculating the temperature drop through the wall of the test section. There are, however, errors in the values of q and k that were substituted into equation (2). The error in measuring the electrical power q

was of the order of ±1 percent, but the leakage of the electric current to the surroundings, which was not taken into account, is estimated to be as much as 2 percent. The value of k_m for the test-section material is estimated to be uncertain to ±7 percent. Consequently the error in the calculated value for the inside surface temperature of the test section might be as large as 14 percent of the temperature drop through the tube wall. This is deemed to be the maximum probable error in the value $t_o - t_s$.

The uncertainty in the value of the heat-transfer coefficients calculated by means of equation (3) is primarily a function of the error in the inside surface temperature of the test section, the inside surface area and bulk temperature being known to within ±1 percent. For example, consider run 21.4 (table 1). An uncertainty of 14 percent of the temperature drop through the tube wall causes an error of 7° in the calculated temperature difference $(t_s - t)$. Since the measured temperature difference was 120°, the maximum probable error in the heat-transfer coefficient h is ±6 percent.

The probable error in measuring the weight flow rate of WFNA is ±4 percent and is due to the following uncertainties: (a) Uncertainty caused by the scatter of 2 percent in the coefficient of discharge of the orifice plate, and (b) uncertainty of 2 percent in the values of the density of WFNA due to changes in its composition.

The probable error in the Fanning coefficient of friction is a function of error in the weight-flow measurement, the measured pressure drop, and the accuracy of the specific-weight measurement. The error in the pressure-drop measurement is estimated to be less than 3 percent and that of the specific weight is 2 percent. These uncertainties give an estimated maximum error of ±7 percent in the value of the Fanning friction coefficient.

The uncertainties in the values of the j-modulus and N_{Re} are primarily due to the uncertainties in the physical-property data for WFNA. The j-modulus is a function of the following variables:

$$j = f\left(h, G, c_p^{1/3}, \mu^{2/3}, k^{2/3}\right)$$

Based upon the probable errors presented above for the properties of WFNA the uncertainty in the values of the j-modulus could be as much as 16 percent assuming that the composition of the WFNA was the same as that used in determining the physical-property data. Even larger uncertainties are possible if the composition of the WFNA used in the heat-transfer experiments differed from that used in determining the physical properties.

The Reynolds number N_{Re} is a function of the following variables:

$$N_{Re} = f(G,D,\mu)$$

The maximum probable error in the values of N_{Re} based upon a WFNA of the same composition as that used in determining its viscosity is ±5 percent. For WFNA compositions that are different the uncertainties would be larger.

RESULTS AND DISCUSSION

Results

Heat-transfer data for WFNA flowing through a 24-inch-long Haynes-Stellite Alloy 25 tube (0.539-inch inside diameter) were obtained over the following range of variables:

Heat-flux density, Btu/(sq in.)(sec)	0.13 - 1.4
Pressure, lb/sq in. abs	64 - 165
WFNA inlet temperature, °F	50 - 137
Reynolds number	55,000 - 220,000

The results are presented in table 1.

Heat Balance

The heat transferred to the WFNA was determined by two methods: (a) By measuring its weight flow rate and its bulk-temperature change and then applying the equation $q = Gc_p(t_2 - t_1)$, and (b) by measuring the electric input with a wattmeter. If heat losses are neglected these two measurements should be equal. Figure 4 is a plot of the heat input to the test section measured electrically as a function of the heat transfer based on method (a). It can be seen from figure 4 that most of the measurements agree within ±5 percent. The large deviations which occurred at small values of bulk-temperature difference are believed to be due to inaccuracies in measuring the bulk temperature. The inaccuracies in measuring the weight rate of flow of WFNA, combined with uncertainties in its specific-heat data, probably account for some of the scatter in the data. There was also some conduction of electrical current through the WFNA that could not be measured. The heat balance indicates that the current conducted through the WFNA was a small fraction of the total current supplied to the test section.

Correlation of Average Fanning Friction Coefficient

Within the convective heat-transfer regime, the Fanning nonisothermal[1] friction coefficient f_q is consistently less than the Fanning isothermal[2] friction coefficient f_{iso} measured at the same flow rate. For the range of average bulk temperatures listed above, the nonisothermal friction coefficient is related to the isothermal friction coefficient measured at the same Reynolds number by the following expression

$$\frac{f_{iso}}{f_q} = \left(\frac{\mu_{bulk}}{\mu_{wall}}\right)^{0.12} \tag{5}$$

In figure 5 the nonisothermal friction coefficients f_q calculated from experimental pressure-drop data are compared with the friction coefficients f_q calculated by means of the above equation. The maximum deviation in comparison is 7 percent, although the deviation for most of the data is less than 4 percent.

Equation (5) is similar to the expressions in the literature which apply to water and n-butyl alcohol. The general expression employed in the literature for relating f_q to f_{iso} is

$$\frac{f_{iso}}{f_q} = \left(\frac{\mu_{bulk}}{\mu_{wall}}\right)^{m}$$

References 6 and 22 present fluid-friction data on water in which the exponent m of the above equation was found to be 0.14 when applied to a range of mean bulk temperatures from 50° to 150° F. Reference 5, which is also an investigation with water, indicates that the exponent m is 0.13 for a range of bulk temperatures from 60° to 125° F. The results of investigations with n-butyl alcohol presented in reference 3 show that the exponent m is 0.14 when the ratio of viscosities is less than 3. Therefore, the magnitude of the exponent m for WFNA which applies to bulk temperatures from 60° to 145° F is not appreciably different from the values reported which apply to water and n-butyl alcohol. The difference in the value of m may be attributed to the difference in the viscosity properties of the liquids in question.

The value of the exponent m for WFNA was determined graphically from the slope of the logarithmic plot in figure 6. The scatter of the

---

[1]With heat addition.

[2]Without heat addition.

data made it necessary to check the maximum deviation of the data from a mean value before the slope could be established. The values of the isothermal friction coefficients employed in equation (4) were obtained experimentally and are presented in figure 7. The curve marked "experimental" in figure 7 is a plot of the experimental friction coefficient of WFNA as a function of the Reynolds number. The other curves in figure 7 were obtained from the Moody report (ref. 23). The surface finish of the inside of the test section was considered to be similar to the finish of commercial drawn tubing. The experimental values of the friction coefficient are about 6 percent higher than the values presented in reference 23 which apply to commercial tubing.

Correlations of Average Heat-Transfer Coefficients

Correlation based on average bulk temperature.- The forced-convection heat-transfer data for WFNA are summarized in figure 8, which presents the Colburn j-factor, $j = \frac{h}{Mc_p}\left(N_{Pr}\right)^{2/3}$, as a function of the Reynolds number N_{Re}. The heat-transfer coefficient h in the aforementioned relationship for j is the average value for the test section. The physical properties of the WFNA used in calculating j and N_{Re} were evaluated at the arithmetic average for the bulk temperature.

Several of the points in figure 8 lie above the curve (straight line) recommended for correlating the data. Approximately one-third of these test points were obtained when the inside surface temperature of the test section exceeded the saturation temperature of the WFNA so that nucleate boiling may have occurred. Consequently they were not expected to correlate with the purely convective data represented by the correlation curve. The points which lie considerably below the correlation curve were obtained in run 28 after the acid had been circulated through the apparatus for several hours. Figure 9 presents the deviation of the results of runs 27 and 28 from the correlation curve as a function of the time that the acid had been circulated through the apparatus. It is seen that the heat-transfer coefficient decreased with this time. The reason for the significant decrease in the heat-transfer rate is not known definitely at this time. Since scale has been reported in boiling heat-transfer measurements with WFNA and dissociation reactions at elevated temperatures change the properties of the WFNA (ref. 21), the aforementioned deviations from the correlation are attributed to these phenomena. The determination of the effect of scale and/or dissociation of the heat-transfer rate for WFNA requires further investigation. The data for run 28 were extrapolated to zero time and the values corresponding to zero time were taken as the j-modulus corresponding to fresh WFNA and a clean test section.

Figure 10 presents the j-modulus as a function of N_{Re}, neglecting the runs where boiling occurred, and the results of run 28 corrected to clean-tube fresh-acid conditions. The data can be correlated by the equation

$$j = 0.024\left(N_{Re}\right)^{-0.2} \tag{6}$$

or

$$N_{Nu} = 0.024\left(N_{Re}\right)^{0.8}\left(N_{Pr}\right)^{1/3} \tag{6a}$$

where all the physical properties of the WFNA are evaluated at its average bulk temperature.

The maximum deviation of the j-modulus from the correlation curve is 32 and -9 percent. The constant in equation (6) can be changed so that the maximum deviation would be approximately ±20 percent. Such a change, however, places the majority of the points below the correlation curve. Equation (6) is, therefore, considered to be the most satisfactory correlation equation for the data presented in figure 10. Moreover, from the point of view of designing a regenerative cooling system it gives conservative values.

The points which lie farthest above the correlation curve in figure 10 represent the data taken in runs 2, 24, and 29. Each run was made with a different test section and fresh WFNA and was the first run in its respective test section. The test section used for run 24 was also used for runs 25 and 26, but in the latter runs a different charge of WFNA was circulated through the apparatus. Since the data for runs 25 and 26 correlate satisfactorily and no additional data were taken with the test sections used in runs 2 and 29 the discrepancies shown by runs 2, 24, and 29 are probably due to differences in WFNA composition and not to instrument error. Since WFNA is not a pure liquid, but a mixture of nitric acid, nitric oxide, and water, its physical properties are functions not only of its temperature but also of its composition. The effect of acid composition on the behavior of WFNA should be more thoroughly and systematically investigated.

Correlation based on Sieder-Tate equation.- Sieder and Tate (ref. 24) proposed that the ratio $(\mu/\mu_s)^n$ be included in correlation equations such as equation (4). This modification is introduced to correct the equation for the lack of temperature similarity. Figure 11 presents

the parameter $j(N_{Re})^{0.2}$ as a function of (μ/μ_s) for the data obtained in the heat-transfer experiments. Although there is considerable scatter in the data, they do indicate that the slope recommended by Sieder and Tate, $n = 0.14$, is substantially correct.

Figure 12 presents $j/(\mu/\mu_s)^{0.14}$ as a function of N_{Re}. The best straight line on the figure for correlating the data appears to be

$$j/(\mu/\mu_s)^{0.14} = 0.022(N_{Re})^{-0.2} \tag{7}$$

or

$$N_{Nu} = 0.022(N_{Re})^{0.8}(N_{Pr})^{1/3}(\mu/\mu_s)^{0.14} \tag{7a}$$

Neglecting the data taken with dissociated acid or a scaled test section (run 28), the data correlate within 34 and -7 percent. Equation (7) does not give a better correlation of the experimental results than does equation (6). The latter equation has the advantage of simplicity.

Reynolds analogy.- The nonisothermal friction data were correlated with the convective heat-transfer data by utilizing the Reynolds analogy. Employing the method described in reference 25, which permits application of the Reynolds analogy to liquids, predicted values of the Nusselt number were calculated. In figure 13 the experimentally determined Nusselt numbers are compared with the predicted values. The average deviation of the calculated values from the experimental values is approximately 9 percent.

In the application of the Reynolds analogy for liquids, one assumption was utilized in addition to those employed in reference 25 for developing the method. Because of the absence of any data concerning the radial temperature distribution of the fluid it was assumed that the maximum temperature difference in a radial direction at any station in the tube would be the difference between the inside wall temperature and the bulk temperature at the station, assuming that the bulk temperature varies linearly with the length of the tube.

Correlation of local values of heat-transfer coefficient.- The variation of the heat-transfer coefficient h with length along the test section was studied. The local values of the heat-transfer coefficient were measured at seven different locations. At each location the physical properties were determined from the local bulk temperature assuming a linear variation of the bulk temperature with test-section

length. Only those nonboiling trials where the over-all bulk-temperature rise for the test section exceeded 15° F were used in order to limit the analysis to tests of the higher heat-flux densities. The data from runs 2, 24, 28, and 29 were omitted because they scattered to such a degree that they made no contribution to the analysis. Local values of the j-modulus and Reynolds number were calculated for the following positions:

Distance from inlet, in.	Distance/diameter, x/D
3	5.6
6	11.1
9	16.7
12	22.2
15	27.8
18	33.4
21	38.9

The data were plotted at each location and were correlated satisfactorily by the equation

$$j = C\left(N_{Re}\right)^{-0.2} \tag{8}$$

where C is a function of the distance from the inlet to the test section and the x/D value. The values of C for the seven locations are tabulated below:

x/D	C
5.6	0.0246
11.1	.0241
16.7	.0243
22.2	.0240
27.8	.0234
33.4	.0232
38.9	.0230

Figure 14 presents C as a function of the tube diameter from the inlet of the test section. In the same figure are presented results of

investigations at Massachusetts Institute of Technology (ref. 6) and University of California, Los Angeles, (refs. 7 to 9) on high-pressure water. Since the M.I.T. values of C were based on physical properties determined at the local film temperature[3] they are not comparable with the values obtained at Purdue University with WFNA or those obtained at U.C.L.A. with water; the latter two investigations based the value of C on the local bulk temperature. The trend of the M.I.T. results, however, is not influenced by temperature employed for determining the physical property of the water. The U.C.L.A. data indicate that the local heat-transfer coefficient decreases rapidly for the first 40 tube diameters of the test section. Thereafter it increases gradually. The U.C.L.A. investigator attributed the increase in the heat-transfer coefficient after the 40 diameters to the increase in liquid temperature (refs. 7 to 9). The length of the test section used in the WFNA experiments at Purdue University was 44.5 diameters or approximately one-third of the x/D ratio of test section used at U.C.L.A. Consequently, the studies of the effect of x/D could not be made completely comparable with those made at U.C.L.A.

The analysis of the effect of x/D on the heat-transfer coefficients indicates that the constant in equation (4) should probably be modified to 0.023. Thus

$$J = 0.023\left(N_{Re}\right)^{-0.2} \tag{9}$$

Equation (9) can then be used to calculate the heat-transfer rate at any position, being slightly conservative at x/D ratios less than x/D = 50.

Nucleate Boiling

Pressure drop with nucleate boiling.- Figure 20 presents the effect of heat addition on the pressure drop across the length of the test section. In the convective region (without nucleate boiling) increasing the rate of heat transmission decreases the pressure drop, but when nucleate boiling is encountered the pressure drop across the test-section length is increased. Nucleate boiling appears to begin whenever the inside surface temperature of the test section reaches the saturation temperature. The region where boiling is assumed to begin is indicated in figure 14. No satisfactory analytical method was developed for predicting the nonisothermal friction coefficient in the boiling heat-transfer regime.

---

[3]The local film temperature is the arithmetic average of the surface and bulk temperature.

The pressure-drop curves for the boiling regime shown in figure 14 are similar to comparable pressure-drop curves presented in the literature (refs. 7 to 10). The effect of varying the system pressure was not investigated in the boiling regime because the heat-flux density required for boiling at pressures above 100 lb/sq in. abs could not be attained. The data for the curves presented in figure 15 were obtained when the system pressure was 64.7 lb/sq in. abs and the bulk inlet temperature was held at approximately 80° F. The upper extent of the heat-flux density for each pressure-drop curve was determined by the maximum tolerated tube-surface temperature at the downstream end of the test section, which was approximately 550° F.

The rapid rise in the pressure drop across the test section with increasing heat flux after boiling begins is attributed to the occurrence of boiling over a greater portion of the inside surface area of the test section. The phenomenon of boiling is thought to increase the pressure drop because:

(a) The nucleate vapor bubbles which form at the inside surface of the tube impose a drag force on the fluid flow

(b) The formation of vapor at the surface of the tube causes the local value of the kinematic viscosity at the wall to increase, signifying that the viscous forces of the fluid are becoming more prominent at the wall

Nucleate-boiling heat transfer.- Some preliminary investigations were made with heat transfer in the nucleate-boiling region. Efforts to correlate these heat-transfer results by using methods employed by other investigators on different liquids were not successful.

Several investigators (refs. 5 and 7 to 10) obtained satisfactory correlation of their data in the nucleate-boiling region by plotting q/A as a function of the excess temperature $\Delta t_x = t_s - t_{sat}$ at a constant pressure. To calculate the excess temperature of WFNA, the vapor-pressure data, obtained at pressures up to 20 lb/sq in. abs by Dr. W. L. Sibbett and others at Purdue University, were extrapolated to a pressure of 65 lb/sq in. abs as shown in figure 16; the values of vapor pressure based on that extrapolation are open to question. Figure 17 presents the heat-transfer data where nucleate boiling was indicated; q/A is plotted as a function of Δt_x. All of the test points on the figure except one are taken from run 25. The tests points tabulated in figure 17 were not included in the plot because the calculated excess temperatures, which were based on the extrapolated values of vapor pressure, were either zero or negative. It is apparent that no correlation of the nucleate-boiling data could be obtained.

Another method for presenting nucleate-boiling data is to plot the heat-flux density against the temperature difference $t_s - t_{bulk}$ for constant weight flow rate (refs. 1 and 5); it was attempted to correlate the nucleate-boiling data for WFNA on that basis. The results are shown in figure 18. The curves are geometrically similar to those obtained by other investigators with fluids other than WFNA. It is seen that for each weight flow rate the slope of the curve increases sharply as the surface temperature of the tube reaches the saturation temperature, indicating that small increases in the surface temperature result in large increases in heat-transfer rates. The investigations with pure liquids show that the data in the boiling region lie on one curve. The experiments with WFNA show two curves in the boiling region, the curves being approximately 40° F apart. Without more precise data on the vapor-pressure-temperature relationship for WFNA, correlation of WFNA data in the boiling region cannot be expected.

Experience with film boiling.- No effort was made to investigate the limits of stable heat transfer with nucleate boiling, but film boiling was inadvertently encountered in one trial. With a constant weight flow of approximately 2.5 pounds per second, the electrical power supplied to the test section was increased to 52 kilowatts which gave an outside surface temperature of approximately 540° F. The power was then reduced to 48 kilowatts which reduced the outside surface temperature to approximately 500° F. After a very short time the test section failed (burn out). The burn-out condition is noted in figure 18. The tube was burned entirely through about $1\frac{7}{8}$ inches from the outlet end.

CONCLUSIONS

The significant conclusions derived from the study of the heat-transfer and fluid-friction characteristics of white fuming nitric acid (WFNA) flowing in an electrically heated horizontal tube are as follows:

1. Over a range of Reynolds numbers from 55,000 to 220,000 and heat-flux densities from 0.13 to 1.4 Btu/(sq in.)(sec) the Fanning friction coefficient obtained with heat transfer in the absence of nucleate boiling f_q can be related to the isothermal Fanning friction coefficient f_{iso} by the expression

$$\frac{f_{iso}}{f_q} = \left(\frac{\mu_{bulk}}{\mu_{wall}}\right)^{0.12}$$

where μ is the viscosity of the WFNA. The average values of heat-transfer coefficient for the test section are correlated satisfactorily by the equation:

$$j = 0.024\left(N_{Re}\right)^{-0.2}$$

where j is the Colburn factor, N_{Re} is the Reynolds number, and the physical-property data are evaluated at the bulk temperature of the WFNA.

2. The local heat-transfer coefficients decreased slightly as the distance from the inlet to the test section is increased. The decrease is attributed to the formation of the thermal boundary layer. For a fully developed boundary layer (ratio of distance from inlet to tube diameter greater than approximately 50) the following equation gives a more satisfactory correlation than does the equation presented under conclusion 1 above:

$$j = 0.023\left(N_{Re}\right)^{-0.2}$$

where the physical properties of the WFNA are based on the local bulk temperature.

3. Continued circulation of the same acid in the test apparatus reduces the heat-transfer coefficient as much as 25 percent. Whether this is due to scale, dissociation, corrosion, or a combination of the three is not known.

4. When the inside surface temperature of the tube exceeds the saturation temperature of the WFNA the heat-transfer rate and the pressure drop are increased over those predicted by the equations presented under conclusions 1 and 2 above. No satisfactory correlations of data obtained in these preliminary investigations in the nucleate-boiling regime were possible; in the case of the heat-transfer data the uncertainty in the vapor-pressure data was one of the principal causes contributing to the difficulty in correlation.

Purdue University,
Lafayette, Ind., February 11, 1953.

REFERENCES

1. Hatcher, J. B., and Bartz, D. R.: High-Flux Heat Transfer to JP-3 and RFNA; Coke Deposition of JP-3. Preprint No. 119, Am. Rocket Soc., Nov. 28, 1951.

2. Kreith, Frank, and Summerfield, Martin: Heat Transfer From an Electrically Heated Tube to Aniline at High Heat Flux. Prog. Rep. No. 4-88, Contract W-04-200-ORD-455, Ord. Dept. and Jet Propulsion Lab., C.I.T., Feb. 7, 1949.

3. Kreith, Frank, and Summerfield, Martin: Investigation of Heat Transfer at High Heat Flux: Experimental Study of Heat Transfer and Friction Drop with n-Butyl Alcohol in an Electrically Heated Tube. Prog. Rep. No. 4-95, Contract W-04-200-ORD-455, Ord. Dept. and Jet Propulsion Lab., C.I.T., May 17, 1949.

4. Kaufman, Samuel J., and Isely, Francis D.: Preliminary Investigation of Heat Transfer to Water Flowing in an Electrically Heated Inconel Tube. NACA RM E50G31, 1950.

5. Kreith, Frank, and Summerfield, Martin: Investigation of Heat Transfer at High Heat-Flux Densities: Experimental Study With Water of Friction Drop and Forced Convection With and Without Surface Boiling in Tubes. Prog. Rep. No. 4-68, Contract W-04-200-ORD-455, Ord. Dept. and Jet Propulsion Lab., C.I.T., Apr. 2, 1948. Also Trans. A.S.M.E., vol. 71, no. 7, Oct. 1949, pp. 805-815.

6. Rohsenow, Warren M., and Clark, John A.: Heat Transfer and Pressure Drop Data for High Heat Flux Densities to Water at High Subcritical Pressures. 1951 Heat Transfer and Fluid Mech. Inst., Stanford Univ. Press (Stanford), 1951, pp. 193-209, 269-270.

7. Buchberg, H., et al.: Final Report on Studies in Boiling Heat Transfer. Rep. No. C0024, Contract AT-11-1-Gen-9, U. S. Atomic Energy Comm, and Dept. of Eng., Univ. of Calif., Los Angeles, 1951.

8. Buchberg, H., Romie, F., Lipkis, R., and Greenfield, M.: Heat-Transfer, Pressure Drop, and Burnout Studies With and Without Surface Boiling for De-Aerated and Gassed Water at Elevated Pressures in a Forced-Flow System. Heat Transfer and Fluid Mech. Inst., Stanford Univ. Press (Stanford), 1951, pp. 177-191, 268.

9. Mead, B. R., Romie, F., and Guibert, A. G.: Liquid Superheat and Boiling Heat Transfer. Heat Transfer and Fluid Mech. Inst., Stanford Univ. Press (Stanford), 1951, pp. 209-216, 271.

10. Jens, W. H., and Lottes, P. A.: Analysis of Heat Transfer, Burnout, Pressure Drop, and Density Data for High-Pressure Water. Rep. No. ANL-4627 Chemistry, Argonne Nat. Lab. (Chicago), May 1951.

11. Gunther, Fred C.: Photographic Study of Surface-Boiling Heat Transfer to Water With Forced Convection. Trans. A.S.M.E., vol. 73, no. 2, Feb. 1951, pp. 115-123.

12. Hawkins, George A.: A Brief Review of the Literature on Boiling Heat Transfer. Res. Contract No. AT(11-1)-Gen-9, U. S. Atomic Energy Comm. and Dept. of Eng., Univ. of Calif., Los Angeles, June 1950.

13. Knowles, J. W.: Heat Transfer With Surface Boiling. Canadian Jour. Res., vol. 26, sect. A., no. 4, July 1948, pp. 268-278.

14. Kreith, F., and Summerfield, M.: Investigation of Heat Transfer at High Heat-Flux Densities: Literature Survey and Experimental Study in Annulus. Prog. Rep. No. 4-65, Contract W-04-200-ORD-455, Ord. Dept. and Jet Propulsion Lab., C.I.T., Feb. 20, 1948.

15. McAdams, W. H., Kennel, W. E., Minden, C. S., Carl, Rudolph, Picornell, P. M., and Dew, J. E.: Heat Transfer at High Rates to Water With Surface Boiling. Ind. and Eng. Chem., vol. 41, no. 9, Sept. 1949, pp. 1945-1953.

16. Rohsenow, W. M., and Clark, J. A.: A Study of the Mechanism of Boiling Heat Transfer. Trans. A.S.M.E., vol. 73, no. 5, July 1951, pp. 609-620.

17. Zucrow, M. J., and Beighley, C. M.: Experimental Performance of WFNA-JP-3 Rocket Motors at Different Combustion Pressures. Jour. Am. Rocket Soc., vol. 22, no. 6, Nov.-Dec. 1952, pp. 323-330.

18. Reese, Bruce A., and Graham, Robert W.: Design of Apparatus for Determining Heat Transfer and Frictional Pressure Drop of Nitric Acid Flowing Through a Heated Tube. NACA RM 52D03, 1952.

19. Bernardo, Everett, and Eian, Carroll S.: Heat-Transfer Tests of Aqueous Ethylene Glycol Solutions in an Electrically Heated Tube. NACA WR E-136, 1945. (Formerly NACA ARR E5F07.)

20. Anon.: Haynes Alloys for High Temperature Service. Haynes Stellite Co. (Kokomo, Ind.), 1948.

21. Sibbitt, W. L., St. Clair, C. R., Bump, T. R., Pagerey, P. F., Kern, J. P., and Fyfe, D. W.: Physical Properties of Concentrated Nitric Acid. NACA TN 2970, 1953.

22. McAdams, William H.: Heat Transmission. Second ed., McGraw-Hill Book Co., Inc., 1942.

23. Moody, Lewis, F.: Friction Factors for Pipe Flow. Trans. A.S.M.E., vol. 66, no. 7, Oct. 1944, pp. 671-684.

24. Seider, E. N., and Tate, G. E.: Heat Transfer and Pressure Drop of Liquids in Tubes. Ind. and Eng. Chem., vol. 28, no. 12, Dec. 1936, pp. 1429-1436.

25. Boelter, L. M. K., Martinelli, R. C., and Jonassen, Finn: Remarks on the Analogy Between Heat Transfer and Momentum Transfer. Trans. A.S.M.E., vol. 63, no. 5, July 1941, pp. 447-455.

TABLE 1

RESULTS OF INVESTIGATION OF WHITE FUMING NITRIC ACID

Run	t_1, °F	Average t, °F	P, lb/sq in. abs	G, lb/sec	q measured electrically Btu/sec	q measured by temp. change, Btu/sec	t_o, °F	t_s, °F	N_{Re}	h, $\frac{\text{Btu}}{(\text{hr})(\text{sq ft})(^\circ\text{F})}$	N_{Nu}	j	f_q
2.1	83.3	87.4	90	2.04	7.09	7.08	161	137	109×10^3	1,812	496	2.66×10^{-3}	---
2.2	87.3	93.4	73	1.63	9.10	8.55	191	161	92.5	1,710	465	2.98	---
2.3	88.9	97.0	75	1.60	11.4	10.8	217	181	92.7	1,743	472	3.06	---
2.4	96.2	106.2	75	1.90	17.2	16.2	267	215	119	2,015	541	2.81	---
2.5	98.5	111.8	75	2.37	24.6	26.7	307	236	154	2,540	677	2.74	---
2.6	94.6	100.6	74	1.38	7.51	6.96	188	163	82.3	1,547	417	3.08	---
2.7	93.9	105.4	71	1.35	15.0	13.1	268	224	83.8	1,610	433	3.18	---
2.8	89.1	97.0	69	2.14	14.9	14.2	230	178	124	2,350	636	3.08	---
21.2	81.8	85.8	69	2.27	7.96	7.68	172	145	117	1,780	476	2.36	432×10^{-5}
21.3	83.9	89.8	69	2.29	12.0	11.4	214	175	122	1,800	497	2.36	417
21.4	86.5	94.9	69	2.22	17.0	15.8	267	215	124	1,810	496	2.38	418
21.5	89.8	100.4	69	2.21	20.8	19.8	312	250	129	1,780	486	2.30	390
21.6	94.8	99.6	65	1.24	5.32	5.13	186	164	72.5	1,052	288	2.41	450
21.7	97.3	105.3	65	1.19	8.68	8.09	234	206	72.8	1,095	297	2.54	468
21.8	98.3	109.4	65	1.17	12.1	11.0	287	251	74.2	1,090	294	2.52	451
21.9	100.0	115.5	65	1.13	16.5	14.9	329	282	75.7	1,270	342	2.85	516
21.12	88.7	93.0	67	2.94	10.7	10.5	194	158	162	2,100	576	2.11	416
21.13	90.0	97.4	67	2.93	19.0	18.4	265	207	167	2,210	605	2.18	404
21.14	91.5	101.5	67	2.91	26.0	24.8	323	248	172	2,260	616	2.20	400
21.15	90.9	96.9	65	1.70	8.91	8.64	207	178	96.9	1,405	385	2.39	427
21.16	91.6	100.3	65	1.70	12.9	12.3	256	216	99.4	1,422	388	2.38	468
21.17	92.9	104.9	65	1.68	18.6	17.2	318	267	102	1,495	405	2.52	464
22.2	80.7	86.4	67	3.30	12.1	16.3	192	152	171	2,360	652	2.19	432
22.3	83.3	91.3	67	3.29	19.0	22.2	248	189	179	2,475	680	2.24	407
22.4	85.4	94.6	66	3.28	22.8	25.3	284	216	183	2,386	655	2.13	411
22.5	87.5	98.7	66	3.27	30.0	31.2	342	257	189	2,420	661	2.13	397
22.6	85.8	90.8	65	2.59	9.21	10.9	184	153	140	1,883	520	2.17	440
22.7	86.5	92.0	65	2.58	12.1	12.0	212	173	141	1,910	527	2.20	432
22.8	87.6	95.2	65	2.58	15.6	16.7	245	196	145	1,980	543	2.24	422
22.9	88.8	97.6	66	2.56	18.6	19.0	275	218	146	1,965	537	2.22	428
22.10	90.0	100.0	66	2.55	22.2	21.8	310	245	149	1,950	532	2.17	420
23.2	60.9	67.6	65	3.00	17.8	17.0	236	180	132	2,020	572	2.27	434
23.3	63.2	73.2	65	2.99	26.0	25.2	309	233	138	2,075	583	2.27	419
23.4	66.0	73.8	65	1.37	8.91	9.08	204	174	63.9	1,131	317	2.68	458
23.5	67.8	81.9	65	1.35	15.7	16.1	302	256	67.4	1,154	321	2.68	562

TABLE 1.- Concluded

RESULTS OF INVESTIGATION OF WHITE FUMING NITRIC ACID

Run	t_1, °F	Average t, °F	P, lb/sq in. abs	G, lb/sec	q measured electrically Btu/sec	q measured by temp. change, Btu/sec	t_o, °F	t_s, °F	N_{Re}	h, $\frac{\text{Btu}}{(\text{hr})(\text{sq ft})(^\circ\text{F})}$	N_{Nu}	J	f_q
24.2	50.5	54.4	65	3.11	11.1	10.3	152	114	124×10^3	2,380	681	2.87×10^{-3}	---
24.3	56.3	68.7	65	3.04	35.6	31.9	353	254	138	2,455	691	2.77	---
24.4	54.9	61.8	67	3.05	19.9	17.9	232	169	130	2,375	675	2.88	---
24.5	58.1	68.2	67	3.08	28.2	26.3	302	219	138	2,380	672	2.68	---
24.7	69.3	91.3	165	2.72	56.9	50.6	487	346	149	2,345	685	2.89	---
24.8	68.3	84.3	114	2.67	41.0	36.9	419	304	138	2,380	661	2.76	---
25.2	79.8	97.8	163	2.76	45.9	42.1	471	357	161	2,265	618	2.32	313×10^{-5}
25.3	79.5	91.7	163	2.77	30.5	28.7	377	294	154	1,926	530	2.04	333
25.5	84.2	98.2	64	2.65	33.9	31.5	396	306	156	2,090	571	2.22	324
25.6	89.0	109.2	64	2.60	47.2	44.4	467	349	165	2,520	680	2.58	421
25.7	90.9	112.0	64	2.58	50.4	46.2	484	360	168	2,600	702	2.63	457
25.8	91.8	109.2	64	2.59	41.0	38.0	459	356	165	2,120	573	2.18	423
25.9	88.5	104.5	64	1.63	24.5	22.1	380	313	101	1,495	406	2.49	462
25.10	91.5	113.0	64	1.60	32.2	29.2	447	365	105	1,633	440	2.65	559
25.11	92.3	115.8	66	1.65	34.9	32.8	483	397	110	1,588	426	2.47	561
26.2	91.0	110.7	75	0.93	17.0	15.6	360	313	60.0	1,070	289	3.03	---
26.3	94.9	122.0	66	0.80	21.2	18.4	391	333	55.7	1,285	343	3.98	---
27.2	84.9	95.8	66	2.30	21.0	21.3	299	237	131	1,904	522	2.39	478
27.3	84.0	97.0	66	2.26	25.4	24.9	340	269	131	1,890	518	2.39	572
27.4	88.0	107.6	66	2.21	37.9	36.8	399	299	140	2,536	687	3.07	652
27.5	86.1	92.4	66	2.21	11.1	11.9	208	172	123	1,779	489	2.36	592
27.6	89.7	105.6	66	2.19	30.0	29.6	372	290	136	2,072	568	2.56	558
27.7	88.6	94.4	66	1.47	6.67	7.13	183	161	83.2	1,275	350	2.52	652
27.8	90.0	99.6	66	1.45	11.3	11.8	249	214	85.9	1,263	345	2.44	616
27.9	88.8	100.8	66	1.45	14.9	14.7	294	250	86.7	1,273	347	2.45	591
27.10	89.1	103.4	66	1.44	18.2	17.5	324	273	87.6	1,370	372	2.62	625
27.11	90.1	112.3	66	1.43	27.7	26.9	379	304	93.0	1,845	497	3.39	736
28.2	82.2	90.3	115	3.78	25.0	25.8	304	232	208	2,297	623	1.77	347
28.3	81.4	87.0	115	3.78	16.9	17.8	237	184	202	2,221	615	1.78	361
28.4	86.1	100.1	115	3.78	45.3	44.5	457	343	223	2,381	650	1.78	343
28.5	85.2	94.3	115	2.77	20.9	21.4	310	250	159	1,716	471	1.78	375
28.6	86.5	98.2	115	2.75	27.3	27.2	377	303	163	1,704	466	1.73	386
28.7	87.2	97.8	115	1.63	14.9	14.7	299	256	96.0	1,200	328	2.07	383
28.8	84.2	89.2	165	3.77	14.8	15.8	231	184	204	1,974	549	1.57	367
28.9	85.6	92.5	165	3.77	20.9	22.1	293	232	211	1,912	526	1.48	350
28.10	85.8	91.0	165	2.49	10.3	10.8	210	177	138	1,532	422	1.81	395
28.11	86.9	95.2	165	2.48	17.1	17.5	287	237	142	1,541	483	1.79	375
28.12	136.8	143.0	65	2.18	7.85	11.4	256	211	171	1,464	383	1.57	502
28.13	135.2	143.8	65	2.15	13.3	15.8	290	250	172	1,592	416	1.70	507
28.14	136.9	147.8	65	1.99	17.5	18.4	332	283	162	1,653	430	1.99	583
28.15	128.5	140.3	65	1.46	13.1	14.6	308	265	114	1,343	352	2.14	753
29.1	63.7	72.1	65	2.54	19.7	18.0	247	186	119	2,244	624	2.93	---
29.2	66.5	79.0	65	2.50	28.0	26.5	324	243	122	2,220	612	2.85	---

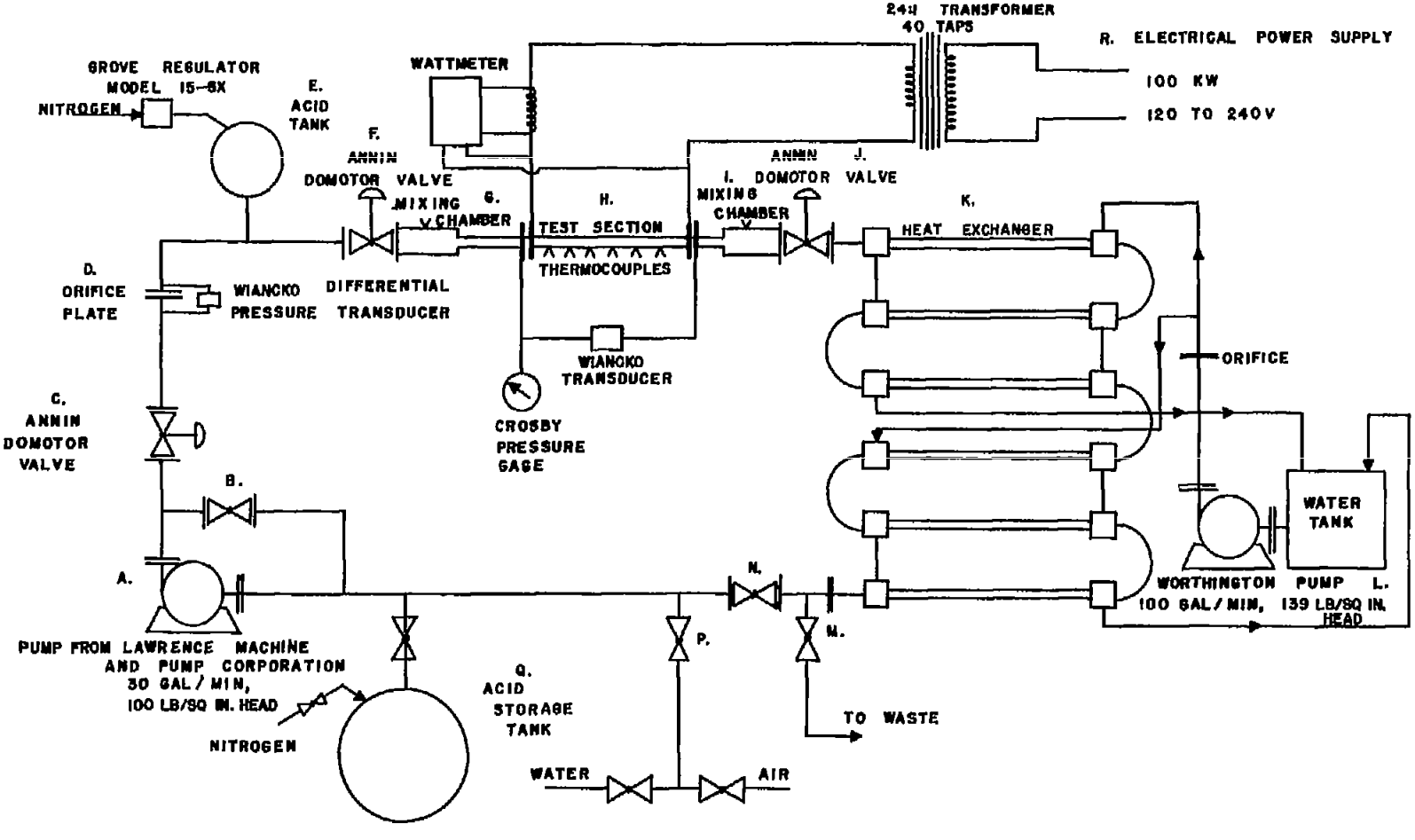

Figure 1.- Schematic diagram of test apparatus.

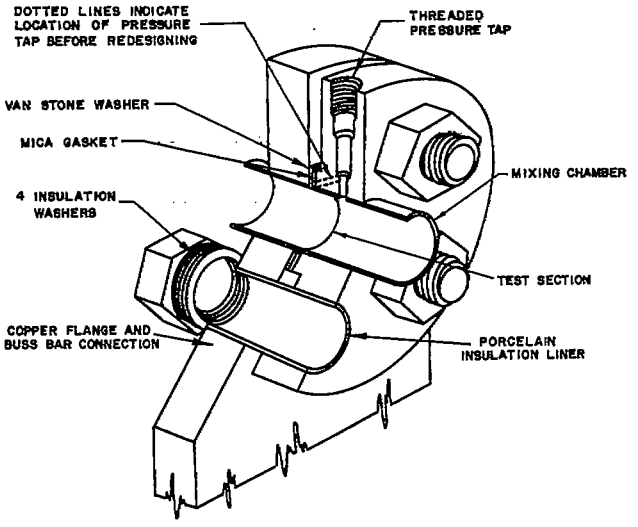

(a) Cross section of flange.

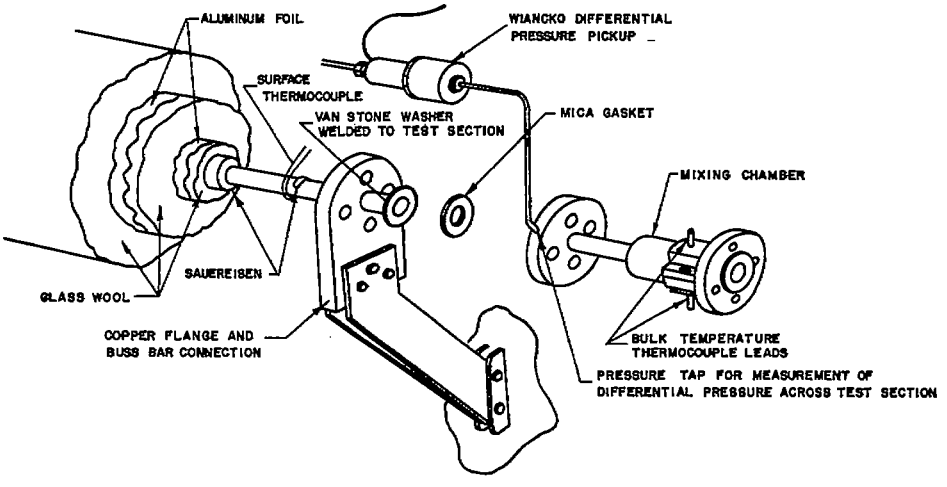

(b) Exploded view of inlet.

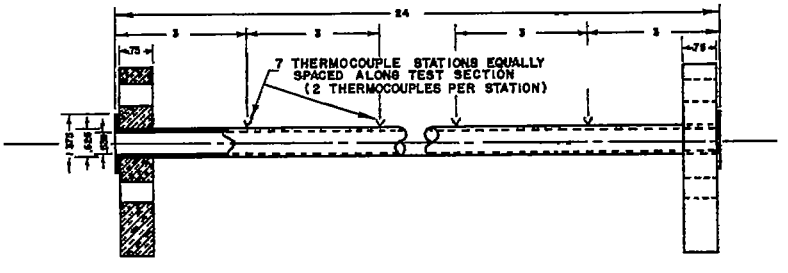

(c) Test section.

Figure 2.- Detail of test-section installation.

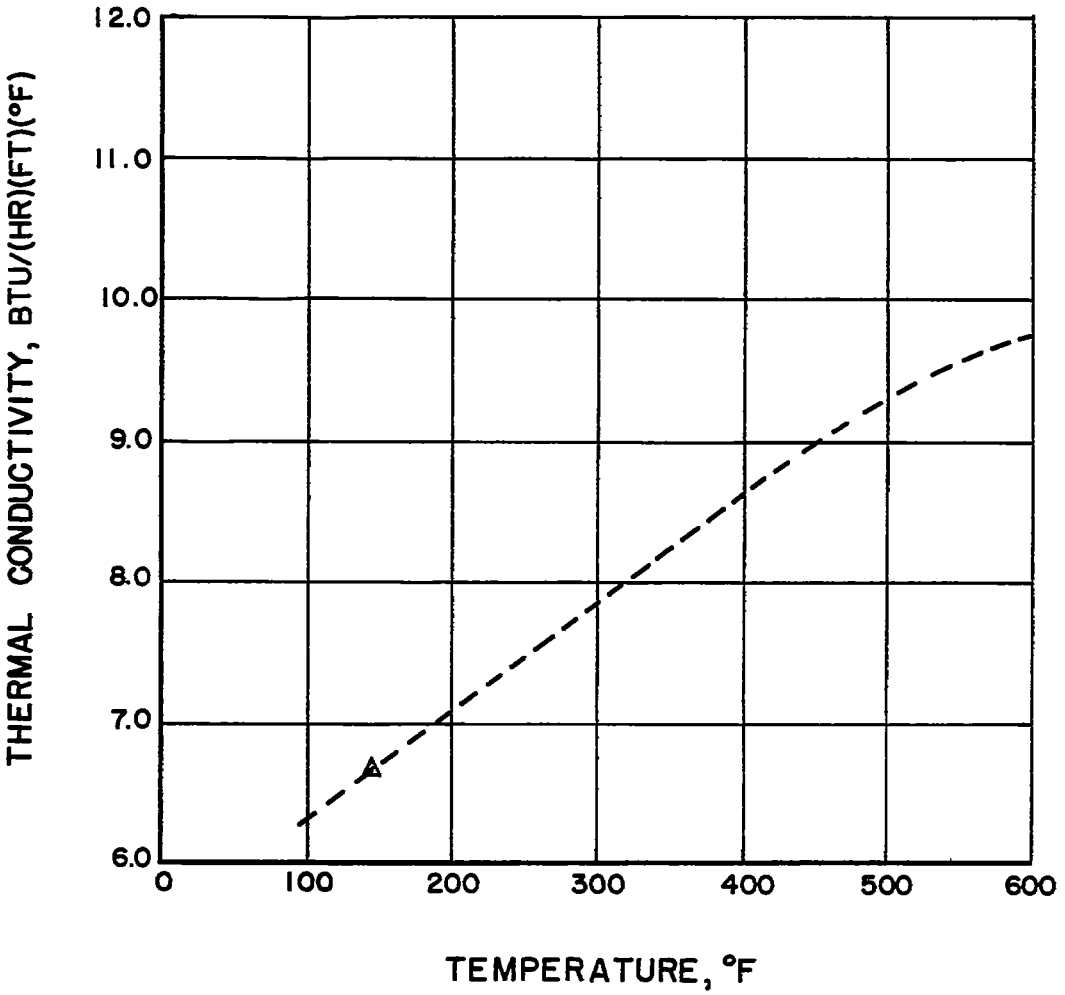

Figure 3.- Thermal conductivity of Haynes-Stellite Alloy 25. Slope based on data for similar alloys from reference 20; experimental point from specific-heat determination.

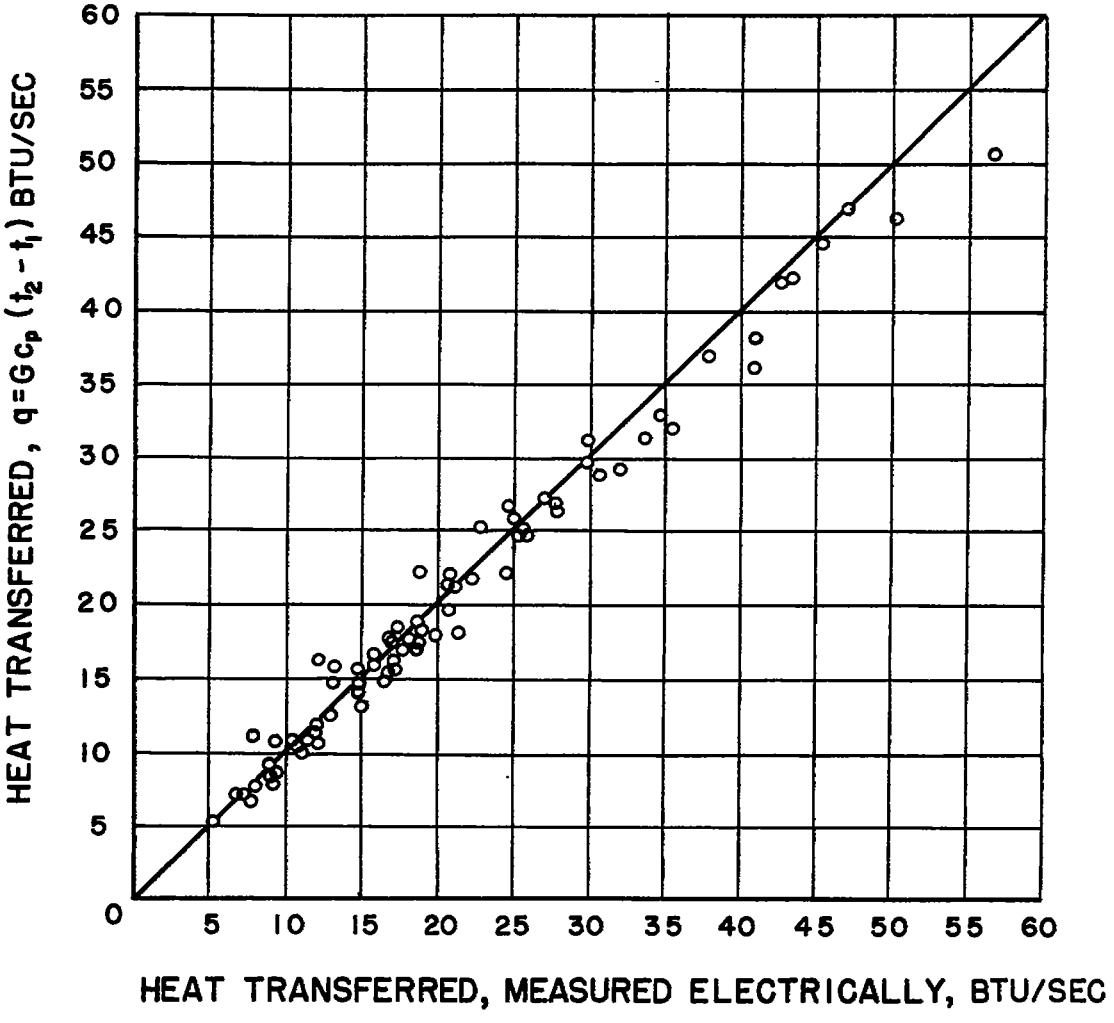

Figure 4.- Heat balance.

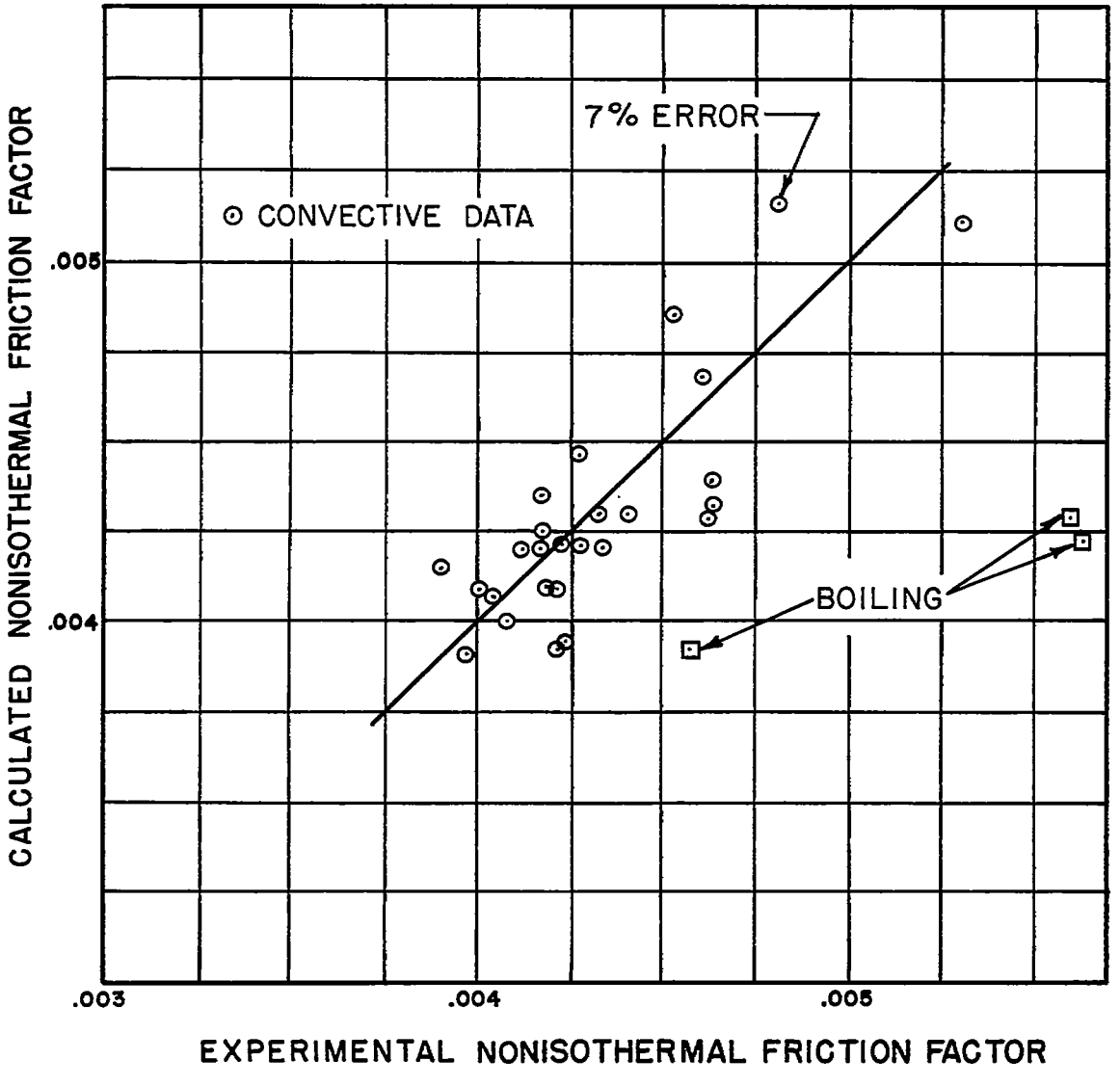

Figure 5.- Comparison between calculated and experimental friction factors.

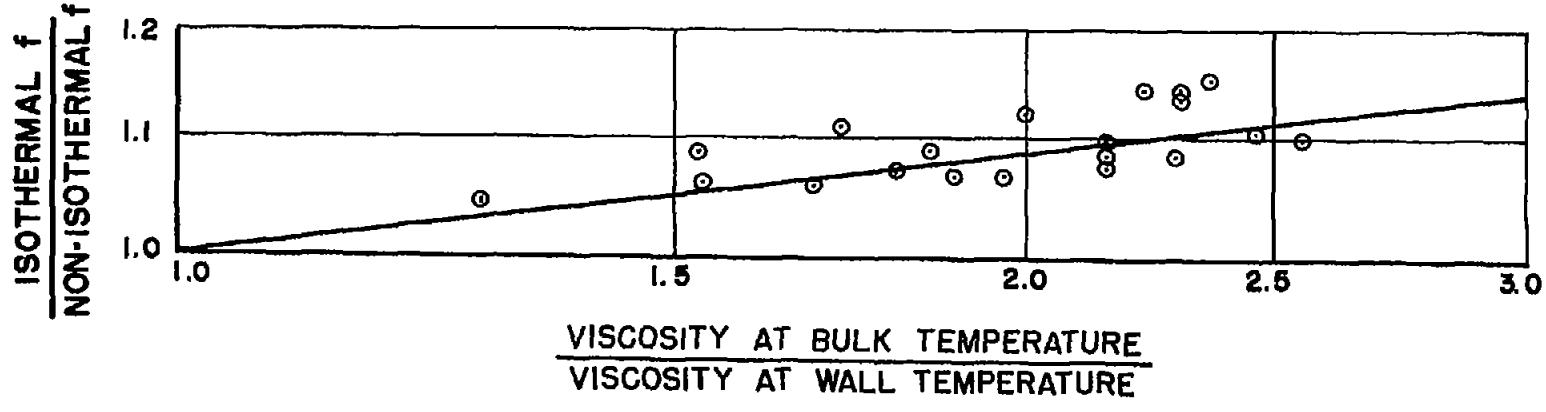

Figure 6.- Relationship between isothermal f and nonisothermal f within convective-heat-transfer region. Average slope, 0.12.

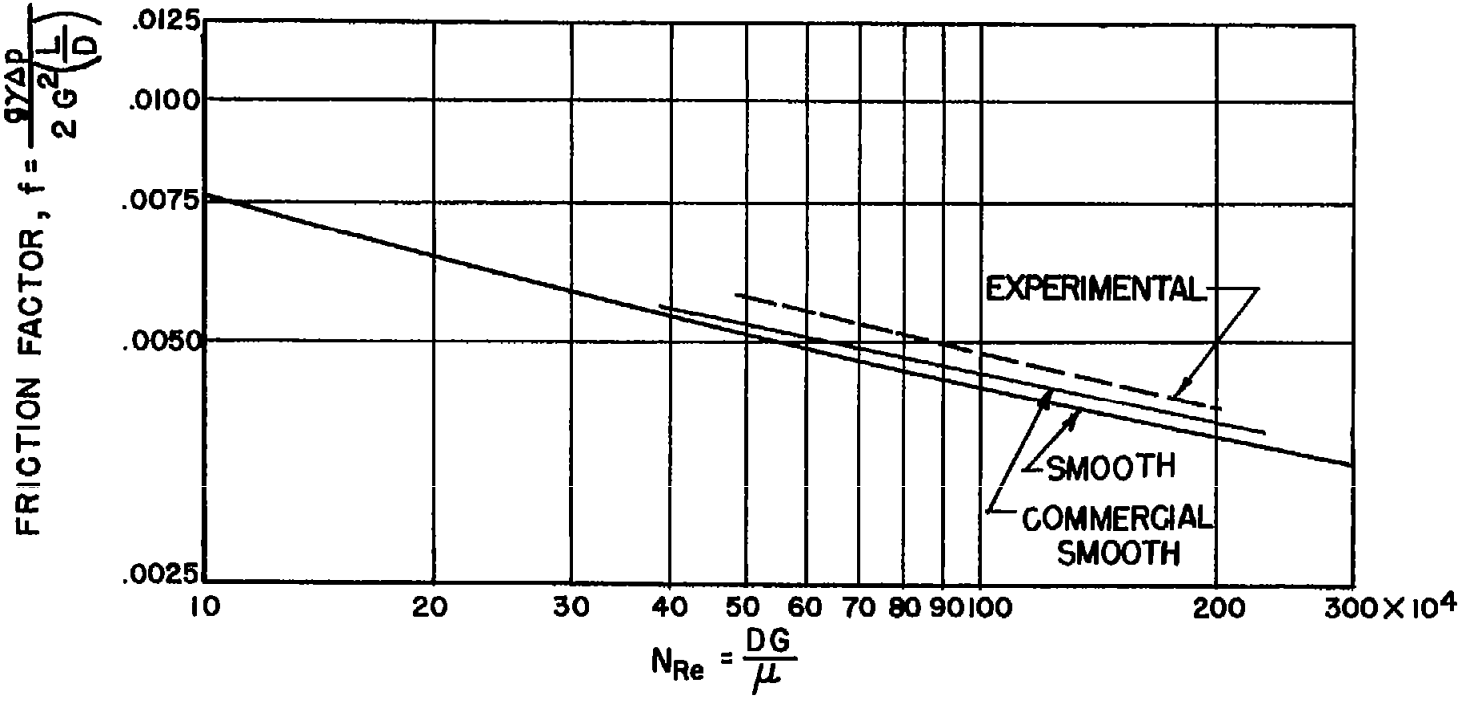

Figure 7.- Isothermal Fanning friction factor for a smooth pipe taken from reference 23.

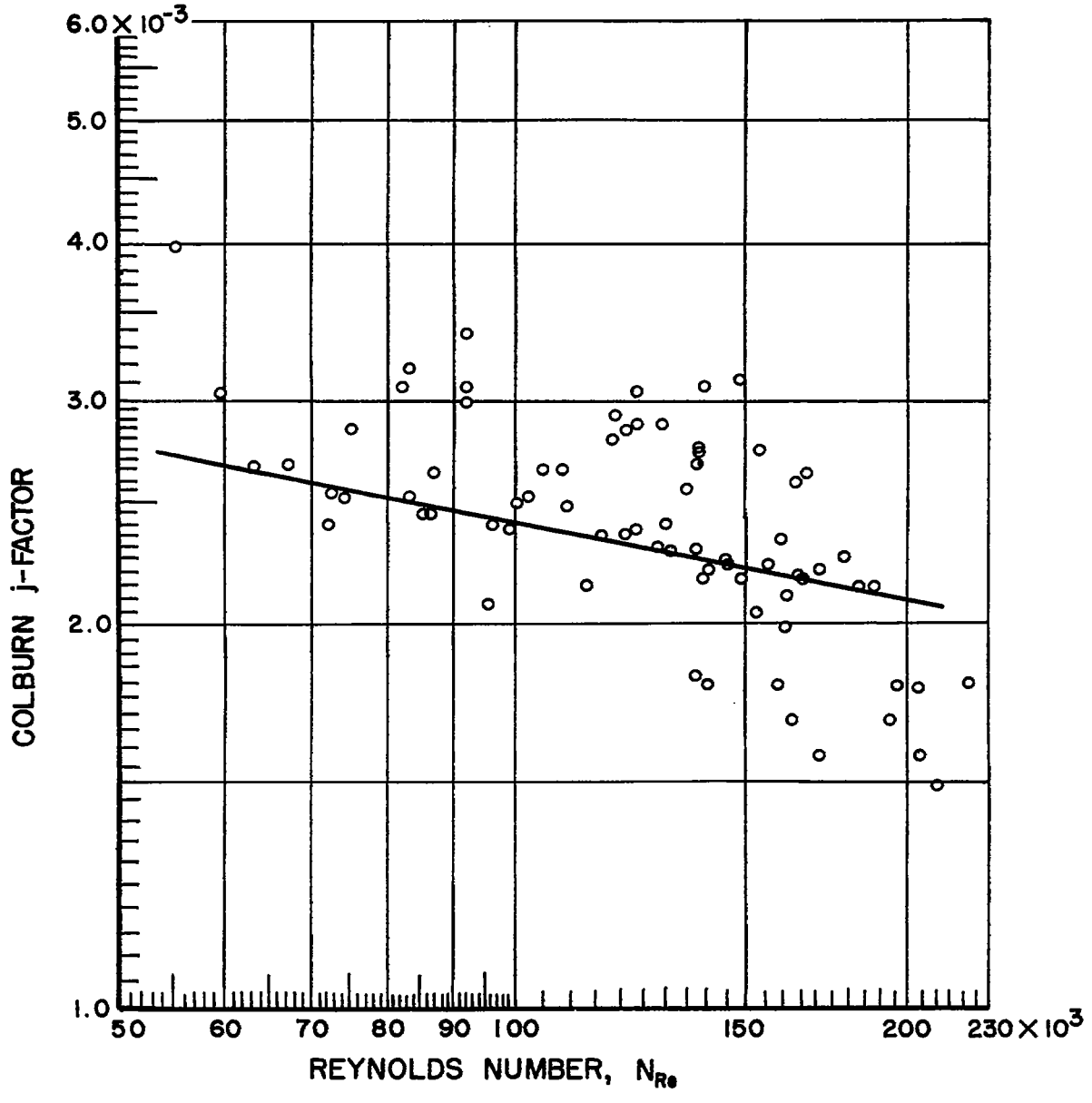

Figure 8.- Correlation of heat-transfer data. Haynes-Stellite Alloy 25 tube 24 inches long with 0.539-inch inside diameter; pressure, 64 to 165 lb/sq in. abs; t_1, 50° to 137° F; physical properties of acid determined at average bulk temperature. Line represents equation $j = 0.024\left(N_{Re}\right)^{-0.2}$.

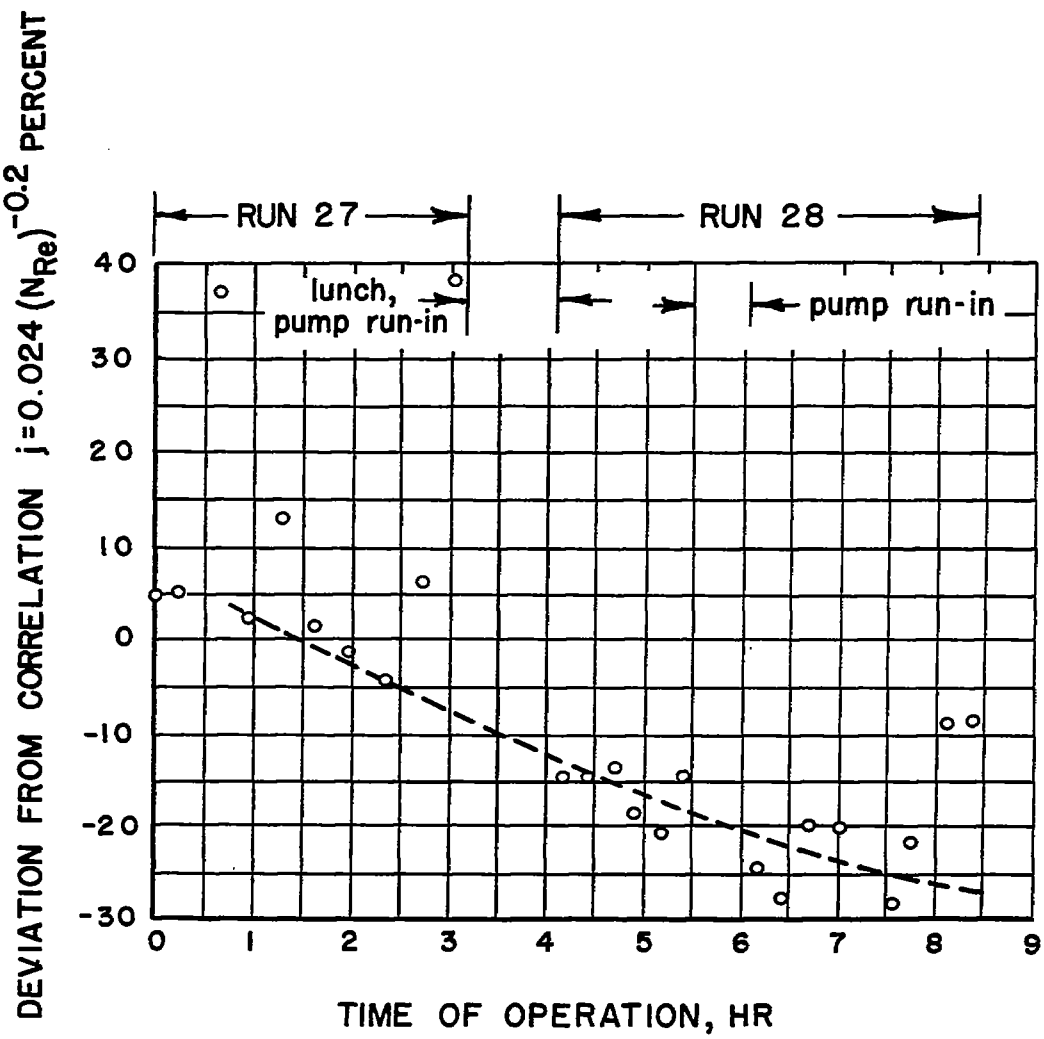

Figure 9.- Effect of scale and/or dissociation on heat-transfer correlation; runs 27 and 28.

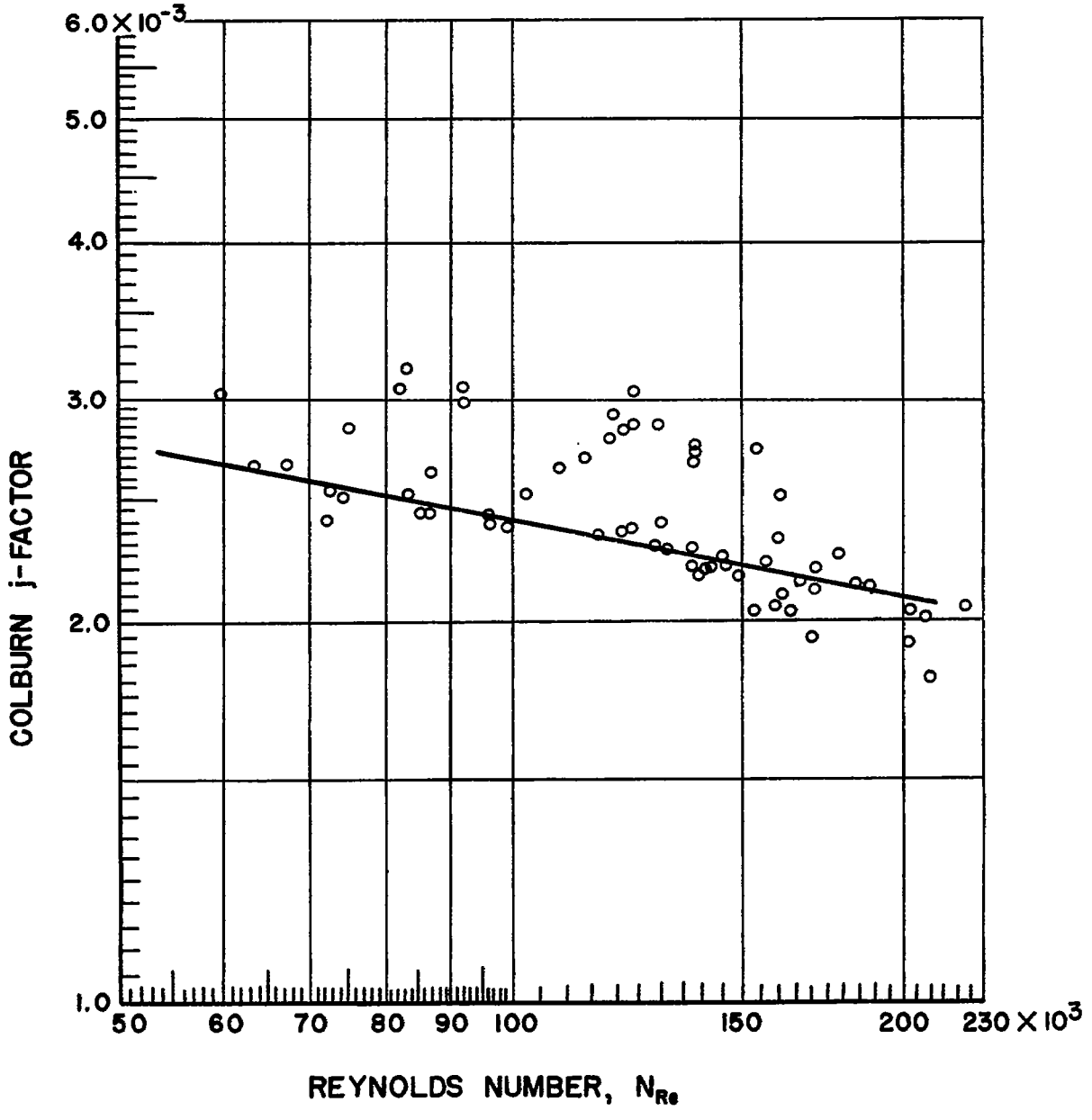

Figure 10.- Correlation of heat-transfer data. Line represents equation $j = 0.024\left(N_{Re}\right)^{-0.2}$; for conditions, see figure 8.

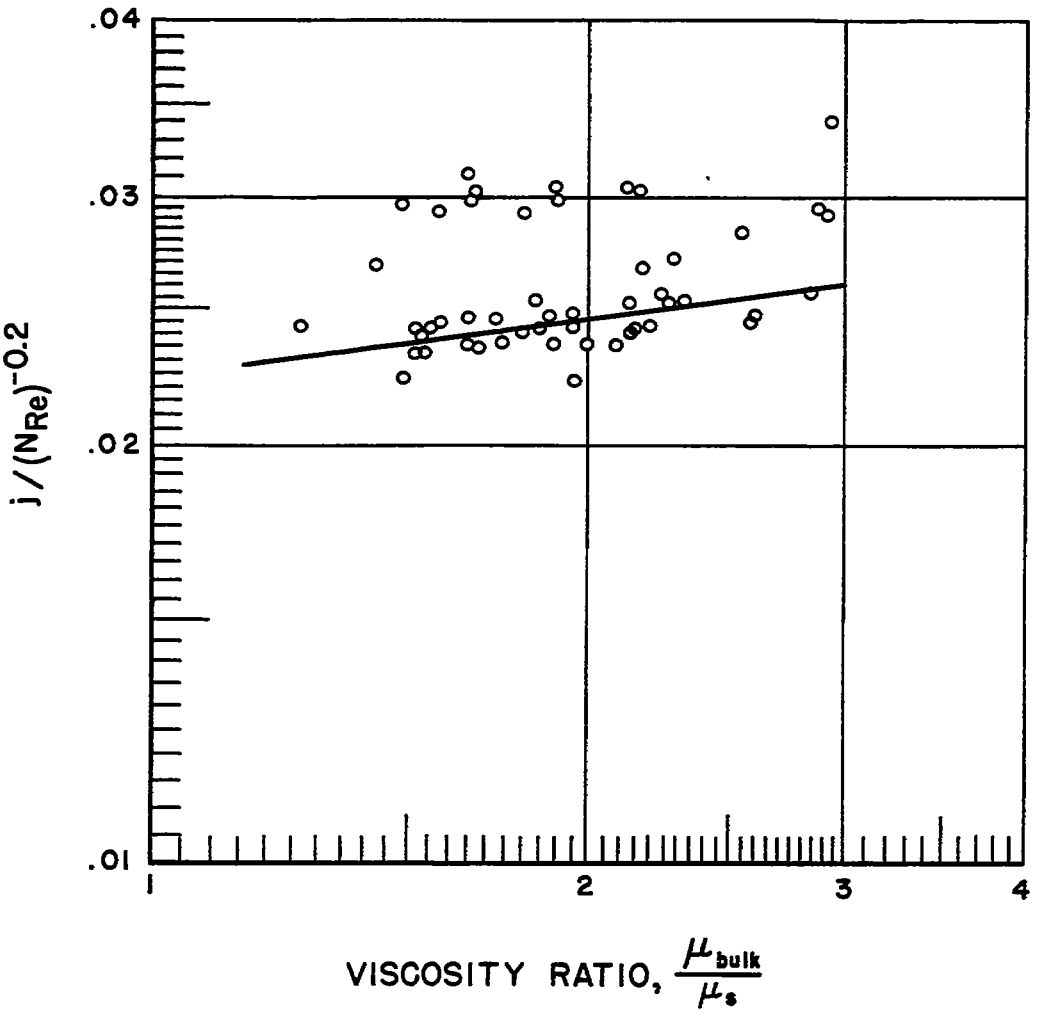

Figure 11.- Influence of viscosity ratio on heat-transfer correlation. Slope, 0.14.

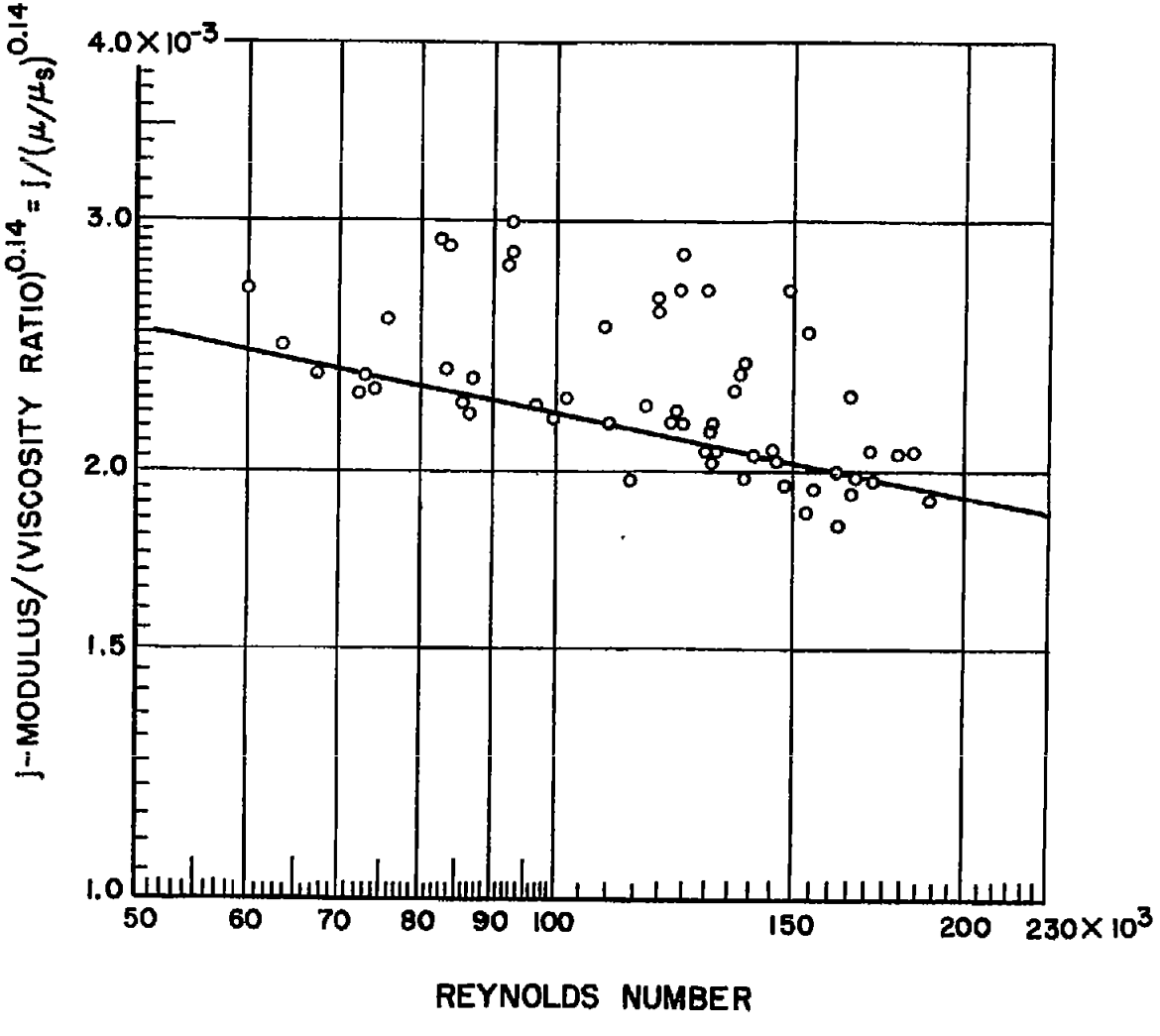

Figure 12.- Correlation of heat-transfer data using viscosity-ratio correction. Line represents equation $j/(\mu/\mu_s)^{0.14} = 0.022(N_{Re})^{-0.2}$; for conditions, see figure 8.

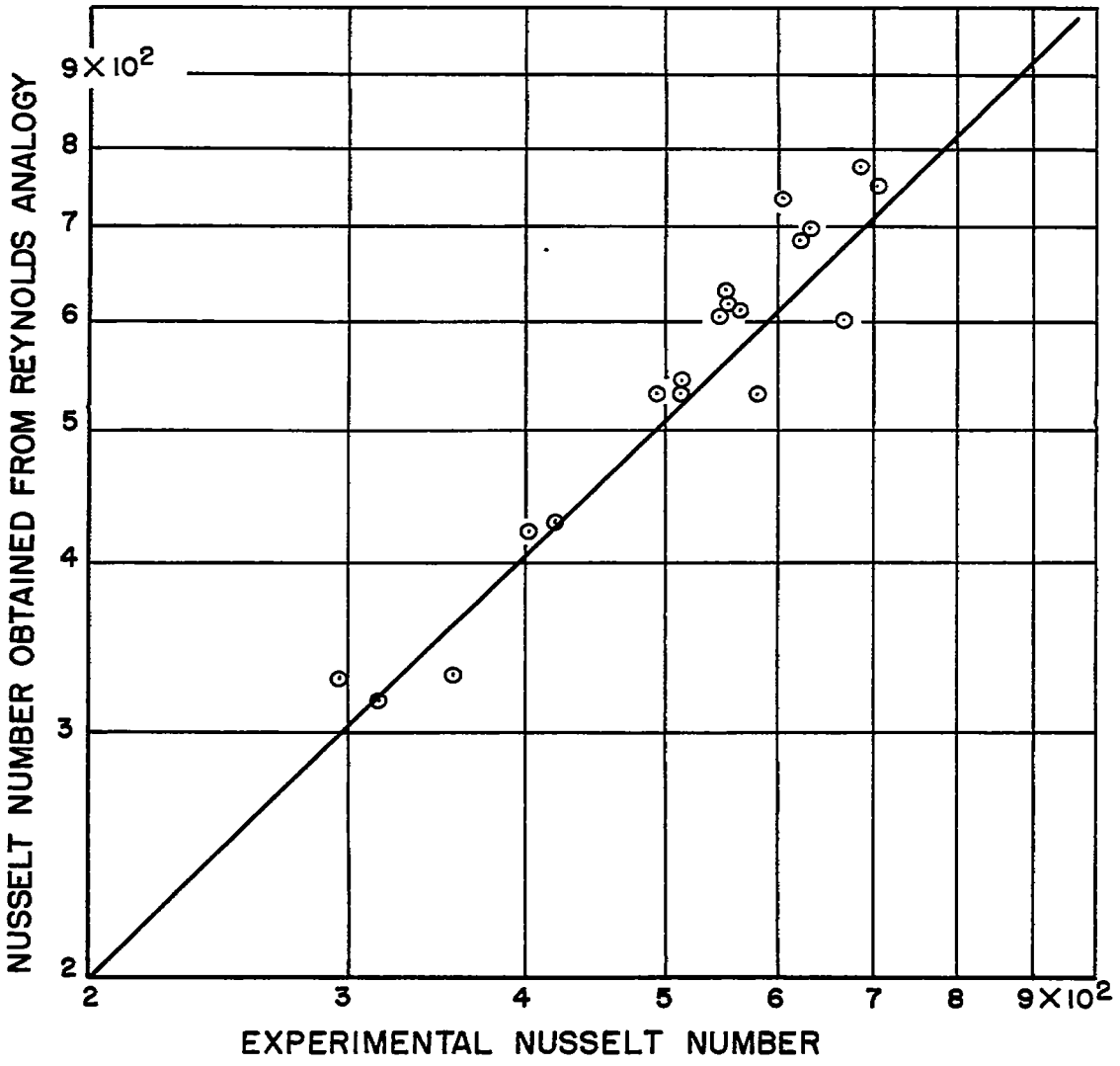

Figure 13.- Relationship between experimental Nusselt number and Nusselt number obtained from Reynolds analogy.

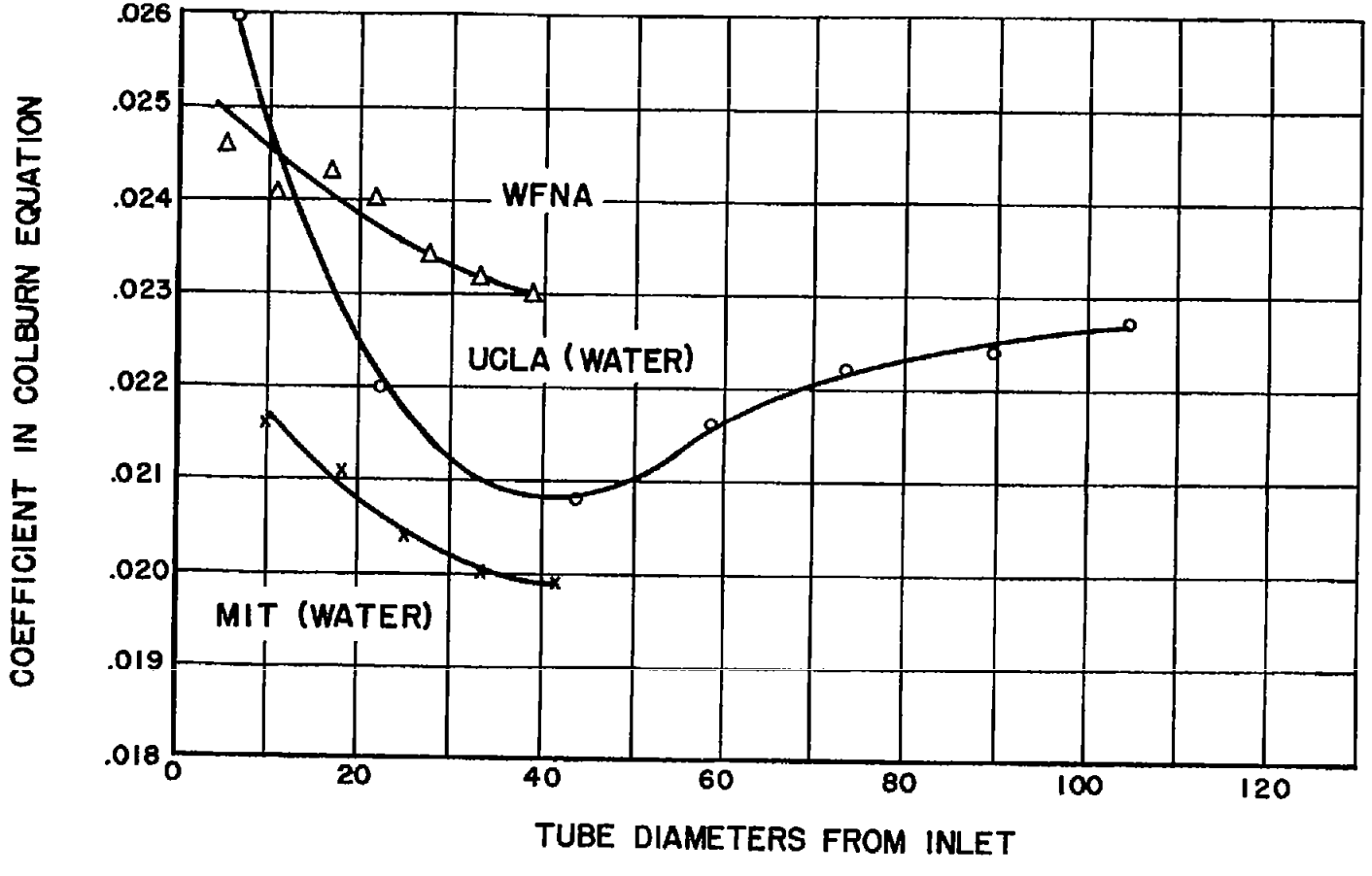

Figure 14.- Effect of L/D ratio on heat-transfer correlation. Data taken from references 7 to 10; coefficient determined by UCLA for WFNA using liquid physical properties determined at bulk temperature and by MIT using film temperature.

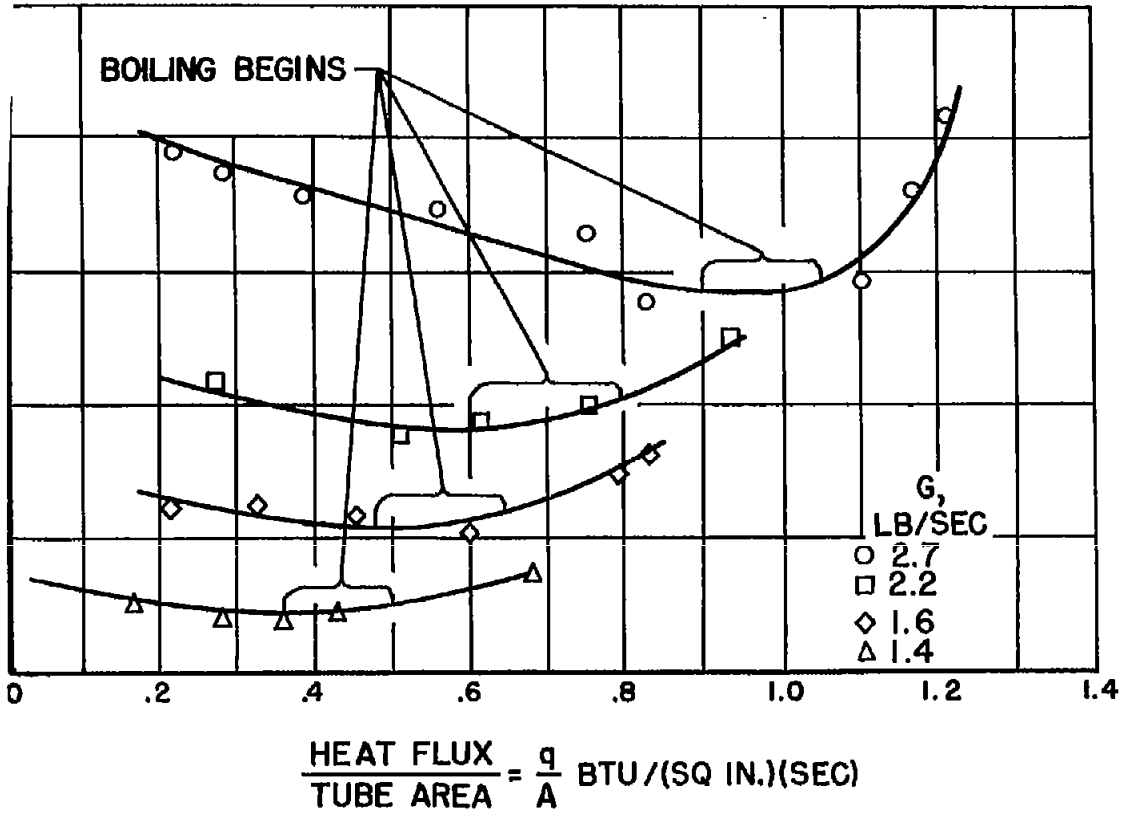

Figure 15.- Effect of heat addition on frictional pressure drop for convective and boiling heat transfer. $t_1 = 80^\circ$ F; P = 64.7 lb/sq in.

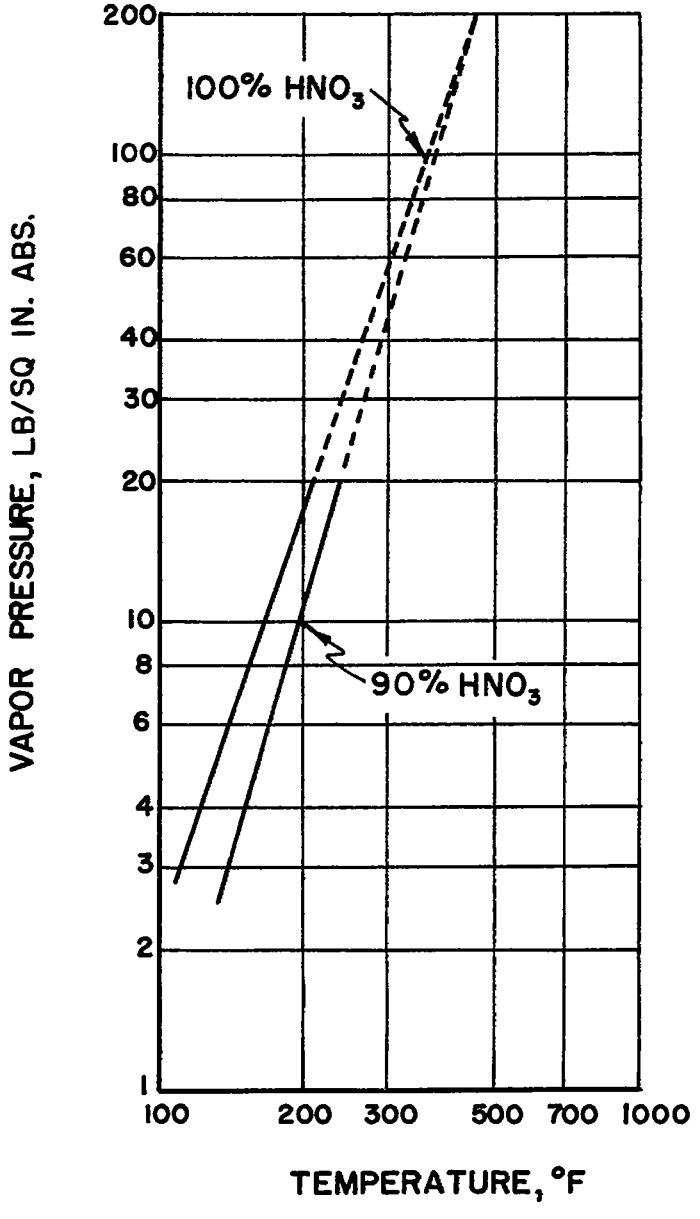

Figure 16.- Extrapolation of low-pressure vapor-pressure data from reference 21.

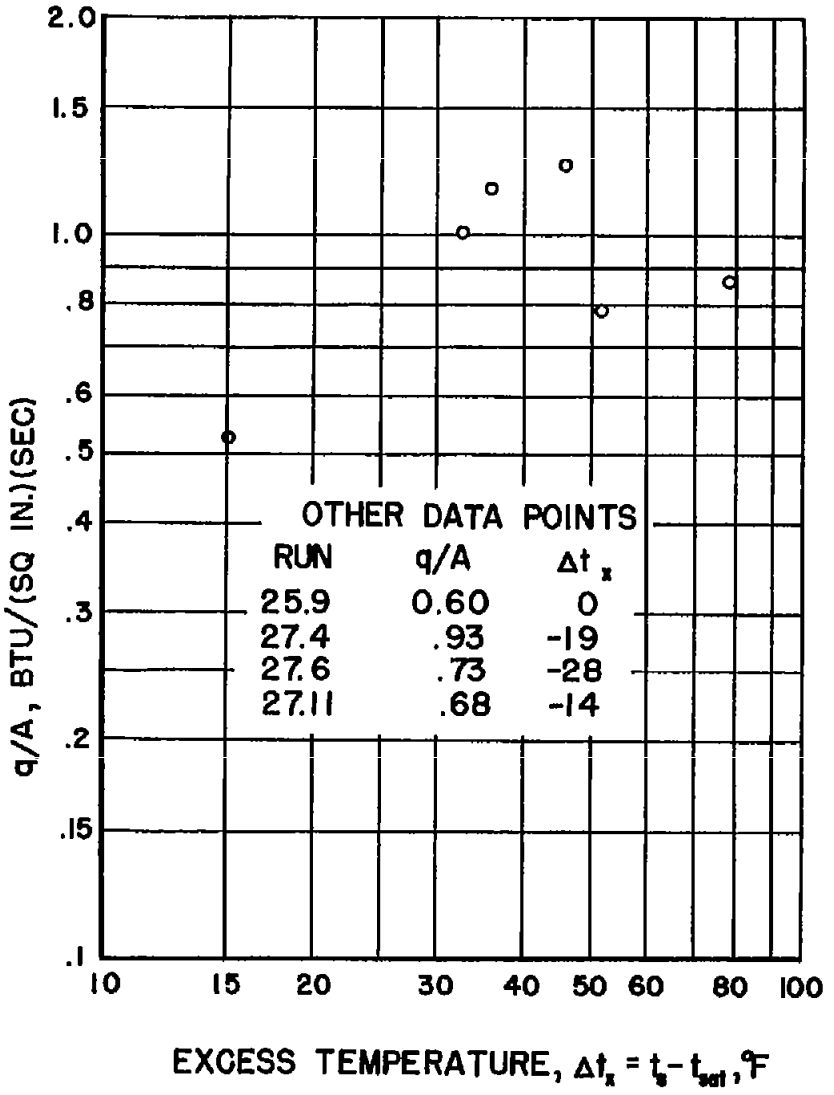

Figure 17.- Effect of excess temperature on nucleate-boiling heat transfer.

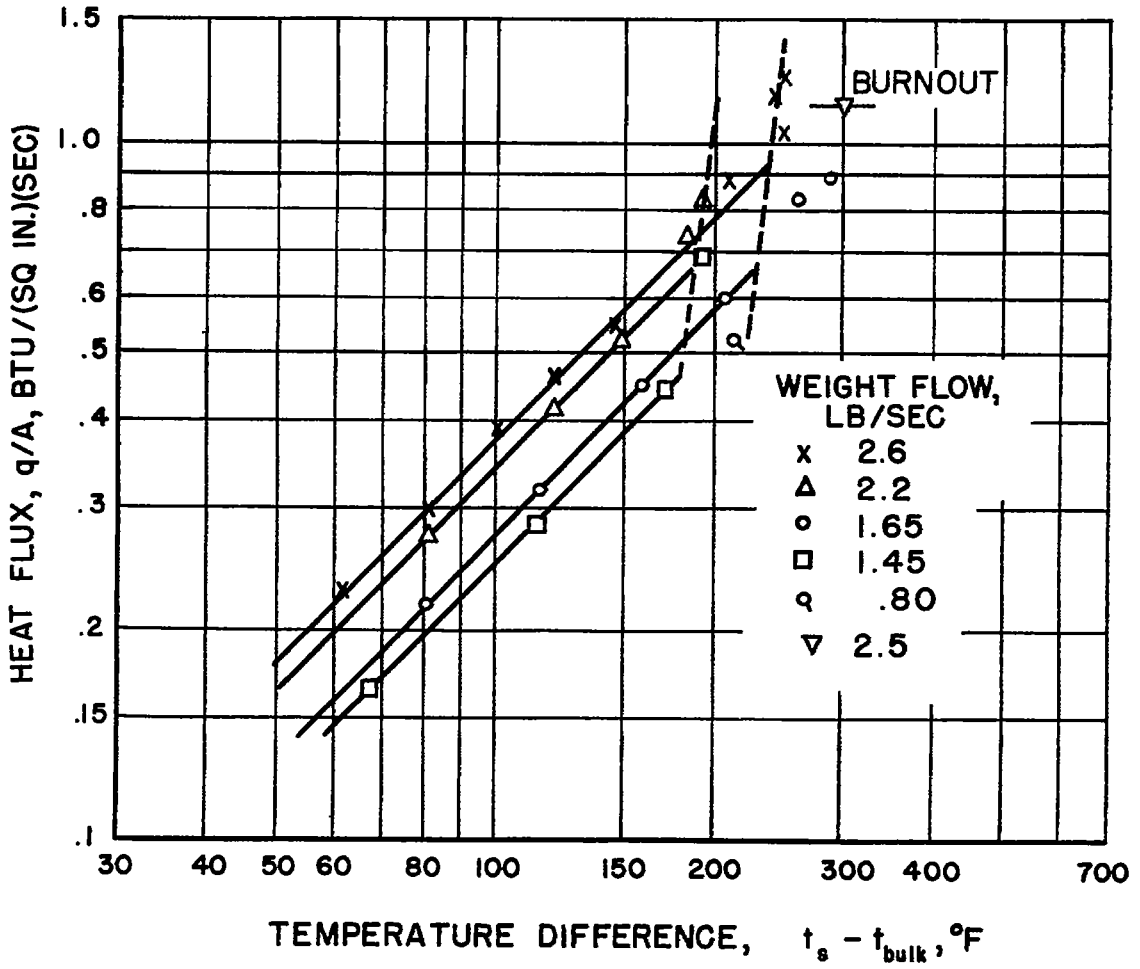

Figure 18.- Forced convection with and without surface boiling. Haynes-Stellite Alloy 25 tube 24 inches long with 0.537-inch inside diameter; t_{bulk}, 91° to 122° F; nucleat boiling pressure, 65 lb/sq in. abs.

NACA-Langley - 5-14-54 - 1000